Quantifying the spatial extent and intensity of recent extreme drought events in the Amazon rainforest and their impacts on the carbon cycle

Phillip Papastefanou[1], Christian S. Zang[1], Zlatan Angelov[1], Aline Anderson de Castro[2], Juan Carlos Jimenez[3], Luiz Felipe Campos De Rezende[2], Romina Ruscica[4,5,6], Boris Sakschewski[7], Anna Sörensson[4,5,6], Kirsten Thonicke[7], Carolina Vera[4,5,6], Nicolas Viovy[8], Celso Von Randow[2] and Anja Rammig[1]

[1] Technical University of Munich, TUM School of Life Sciences Weihenstephan, Freising, Germany

[2] Earth System Sciences Centre, National Institute for Spatial Research, São José dos Campos, São Paulo, Brazil

[3] GCU/IPL, University of Valencia, Valencia. Spain.

[4] Universidad de Buenos Aires, Facultad de Ciencias Exactas y Naturales, Departamento de Ciencias de la Atmósfera y los Océanos. Buenos Aires, Argentina.

[5] CONICET – Universidad de Buenos Aires. Centro de Investigaciones del Mar y la Atmósfera (CIMA). Buenos Aires, Argentina.

[6] CNRS – IRD – CONICET – UBA. Instituto Franco-Argentino para el Estudio del Clima y sus Impactos (UMI 3351 IFAECI). Centro de Investigaciones del Mar y la Atmósfera (CIMA). Buenos Aires, Argentina.

[7] Potsdam Institute for Climate Impact Research (PIK), Telegraphenberg A31, Potsdam, 14473, Germany

[8] LSCE, CEA-CNRS-Univ Paris-Saclay, Saclay, France

Correspondence to: Phillip Papastefanou (papa@tum.de)

Abstract. Over the last decades, the Amazon rainforest was hit by multiple severe drought events. Here, we assess the severity and spatial extent of the extreme drought years 2005, 2010, and 2015/2016 in the Amazon region and their impacts on the regional carbon cycle. As an indicator of drought stress in the Amazon rainforest, we use the widely applied maximum cumulative water deficit (~~AMCWD~~MCWD). Evaluating an ensemble of ~~ten~~nine state-of-the-art precipitation datasets for the Amazon region, we find that the spatial extent of the drought in 2005 ranges from 2.~~8~~2 to ~~4.2~~3.0 (mean = ~~3.~~2.7) million km² (~~46 – 71~~37 – 51% of the Amazon basin, mean = ~~53~~45%) where ~~AMCWD~~MCWD indicates at least moderate drought conditions (~~AMCWD~~relative MCWD anomaly < ~~25 mm~~-0.5). In 2010, the affected area was about 16% larger, ranging from 3.~~1~~0 up to 4.~~6~~4 (mean = 3.~~7~~6) million km² (~~52 – 78~~51 – 74%, mean = ~~63~~61%). In 2016, the mean area affected by drought stress was ~~similar to~~between 2005 and 2010 (mean = 3.2 million km²; 55% of the Amazon basin), but the general disagreement between ~~data sets~~datasets was larger, ranging from 2.4 up to 4.1 million km² (40 – ~~70~~69%). In addition, we compare differences and similarities among datasets using the self-calibrating Palmer Drought Severity Index (scPDSI) and a rainfall anomaly index (RAI). We find that scPDSI shows a ~~much~~stronger, and RAI a much weaker drought impact in terms of extent and severity for the year 2016 compared to ~~AMCWD~~MCWD. Using an empirical ~~AMCWD~~MCWD-mortality relationship, we calculate biomass losses ~~of~~for the ~~three~~2005 drought ~~events~~event. We show that ~~eight~~the majority of ~~ten~~the datasets agree on biomass losses of about 1.~~8~~2 Petagram carbon (PgC ~~for the drought years 2005 and 2010, indicating that the more intense drought in 2005 equals a larger total area of the 2010 drought regarding biomass loss. For~~), but the ~~2015/2016 drought event, datasets show a large variability of biomass loss induced by drought stress ranging from~~ overall range is between 0.7 and 1.~~3 to 2.7~~6 PgC ~~with a mean loss of 1.8 PgC.~~. Disagreement across datasets increased, (1) when comparing the total area of ~~more~~ severe and extreme drought signals and (2) when comparing spatial drought location across datasets. ~~Generally, only half of the datasets agreed on the location of a drought event.~~ We conclude that for deriving impacts of droughts ~~to~~on the Amazon Basin based on precipitation, ~~an ensemble of~~multiple datasets should be considered. This is especially relevant when assessing the impact of drought on the Amazon rainforest and its carbon cycle. Furthermore, considering different drought indices can help to understand the complex characteristics that drought events in the Amazon have.

1 Introduction

The severe drought events occurring in 2005, 2010 and 2015/16 in the Amazon basin are reasons for concern regarding their frequency and severity, and their impacts on the Amazon rainforest. Different large-scale atmospheric processes related to increased sea surface temperature (SST) in the Pacific and the Atlantic Ocean seem to be responsible for such repeated mega-drought events (Coelho et al., 2012): While the drought 2015/16 was driven by a record-level El Niño event enhanced by the strong underlying global warming trend (Jimenez et al., 2018), the 2010 drought was a combination of a moderate El Niño event and anomalously warm SSTs in the tropical North Atlantic (Marengo & Espinoza, 2016; Marengo et al., 2011). Similarly, the 2005 drought was attributed to anomalies of warm SSTs in the North Atlantic (Marengo et al., 2008; Zeng et al., 2008). In consequence, such events differ in their strength, their timing and spatial patterns, and thus, impacted regions differ. While drought events related to El Niño events show a Southwest to Northeast gradient with dry conditions over the NE Amazon region (Malhi et al., 2008), drought events caused by anomalously warm North Atlantic SSTs show a North-South gradient with dry conditions in the southern Amazon region (Lewis et al., 2011; Marengo et al., 2008). Even in the case of El Niño events, SSTs anomalies over the Eastern Pacific (EP) or the Central Pacific (CP) can lead to different impacts and spatial patterns of drought (Jimenez et al., 2019). In addition to their influence on temperature, recent El Niño events also showed amplified atmospheric vapor pressure deficit anomalies (Barkhordarian et al., 2019; Rifai et al., 2019). The impacts of such drought events on humid tropical forests, which are often not adapted to longer-lasting dryness, are severe. Increased forest mortality connected to drought events was observed in central and southern Amazonia (Lewis et al., 2011; Phillips et al., 2009), as well as shifts in tree species composition (Esquivel Muelbert et al., 2019). Droughts are assumed to be one of the main drivers for the observed decline in the Amazon carbon sink, indicating that more carbon is lost to the atmosphere than taken up by the forest (Hubau et al., 2020). Thus, such extreme drought events are altering the carbon cycle of the Amazon forest already today (Gloor et al., 2015; Hubau et al., 2020; Phillips et al., 2009).

Losing tropical forests in the Amazon region through increased mortality under drought also has implications for regional and continental-scale water cycling (Ruiz Vásquez et al., 2020). The rainforest transpires enormous amounts of water which is transported by winds to remote regions far beyond the borders of the rainforest (e.g. Dirmeyer et al., 2009; van der Ent et al., 2010; D. C. Zemp et al., 2014; Zemp et al., 2017a). In addition, the ongoing deforestation in the Amazon rainforest further decreases forest cover and thus, transpiration rates, leading to a rainfall decline and enhanced drought conditions in a positive feedback loop (Miralles et al., 2019; D. C. Zemp et al., 2017a; Zemp et al., 2017b). It can be expected that ongoing climate change most likely will cause stronger and more frequent drought events in the Amazon (Cai et al., 2015; Jia et al., 2019; Marengo & Espinoza, 2016).

For assessing the severity, the spatial extent and, in particular, the impacts of such drought events on existing ecosystems, different gridded precipitation datasets are available which in some cases differ strongly in magnitude and spatio-temporal distribution of precipitation amounts (Golian et al., 2019). Typical problems of precipitation data for South America encompass the underestimation of extreme rainfall events in both dry or wet seasons (Blacutt et al., 2015; Giles et al., 2020). Therefore,

while for the Amazon region, the recent drought events have been assessed in terms of severity (Jiménez-Muñoz et al., 2016; Jimenez et al., 2018) and impacts (Phillips et al. 2009, Lewis et al. 2011) based on single precipitation data sets, a systematic analysis of how the most frequent used precipitation datasets differ regarding the spatial extent, location and severity of recent extreme drought events, is currently missing.

For our study, we selected ten precipitation datasets: (1, 2) Data from the Tropical Rainfall Measurement Mission (TRMM) version 6 and 7 (Huffman et al., 2007) which have been frequently used, e.g. to estimate drought impacts on the carbon balance (Lewis et al., 2011; Malhi et al., 2009) and are assumed to represent precipitation patterns in the Amazon region best since they are derived from radar measurements (Huffman et al., 2007). (3) CHIRPS (Climate Hazards group Infrared Precipitation with Stations, Espinoza et al., 2019), which has been used to study regional hydro-climatic and environmental changes in the Amazon Basin. These two datasets only provide precipitation and no information about other climatic variables such as temperature or radiation. In addition, we selected five datasets that are often used as drivers for ecosystem models (e.g. in Forkel et al., 2019; Yang et al., 2015) and – in contrast to the other datasets – provide information about other climate variables: Data from the Climate Research Unit (CRU) with a joint project reanalysis (NCEP, National Centers for Environmental Prediction) applied, (4) the CRUNCEP (version 8, Viovy, 2018), (5) the WATCH-WFDEI (WATCH: Water and Global Change, Weedon et al., 2011. WFDEI: WATCH Forcing Data methodology applied to ERA-Interim, Weedon et al., 2014) dataset, originally derived from global sub-daily observations merged with integrations from a general circulation model, (6) the GSWP3 (Global Soil Wetness phase 3, Kim et al. in prep) dataset which is closely related to WATCH-WFDEI, relying on a similar forcing but with a different bias correction applied, (7) the newer GLDAS s(Global Land Data Assimilation System) 2.1. which is derived from various geostationary infrared satellite measurements and microwave observations (Rodell et al., 2004), (8) the ERA-Interim dataset which is generated using a forecast model driven with different input datasets (Dee et al., 2011), (9) the latest ECMWF atmospheric reanalysis dataset, ERA5, which is the successor of ERA-Interim, providing higher spatial and temporal resolutions and a more recent model and data assimilation system than the previous ERA-Interim reanalysis (Albergel et al., 2018), and, finally, (10) the GPCC (named after the Global Precipitation Climatology Centre) dataset (Schneider et al., 2018), which is based on globally available land stations (rain gauges) combined with an empirical interpolation method (Willmott et al., 1985). A more detailed description of the datasets is given in the methods section.

We evaluate the precipitation datasets based on the Maximum Cumulative Water Deficit (MCWD; Aragão et al., 2007), a well-established drought index that is particularly suitable for estimating drought stress in the Amazon region (e.g. Esquivel-Muelbert et al., 2019; Lewis et al., 2011; Y. Malhi et al., 2009; Phillips et al., 2009; Zang et al., 2020). In addition, we included two other measures to complement our analysis: Rainfall anomaly index (RAI), which does account for the mean deviation (in units of standard deviation) of precipitation during the driest months of the year and scPDSI (self-calibrating Palmer Drought Index, Wells et al., 2004). scPDSI has a more complex formulation compared to RAI and MCWD and takes available soil water content into account. Both RAI and scPDSI have been used in studies describing the recent Amazonian drought events (e.g. Jiménez-Muñoz et al., 2016; Lewis et al., 2011).

255 ~~The goals of our study are (1) to analyze and quantify the uncertainty in drought strength, extent and location of three recent Amazon droughts in the years 2005, 2010 and 2015/2016 in ten state of the art precipitation~~The severe drought events occurring in 2005, 2010, and 2015/16 in the Amazon basin are reasons for concern regarding their frequency and severity, and their impacts on the Amazon rainforest. Different large-scale atmospheric processes related to increased sea surface temperature (SST) in the Pacific and the Atlantic Ocean seem to be responsible for such repeated mega-drought events (Coelho

260 et al., 2012): While the drought 2015/16 was driven by a record-level El Niño event enhanced by the strong underlying global warming trend (Jimenez et al., 2018), the 2010 drought was a combination of a moderate El Niño event and anomalously warm SSTs in the tropical North Atlantic (Marengo & Espinoza, 2016; Marengo et al., 2011). Similarly, the 2005 drought was attributed to anomalies of warm SSTs in the North Atlantic (Marengo et al., 2008; Zeng et al., 2008). In consequence, such events differ in their strength, their timing, and spatial patterns, and thus, impacted regions differ. While drought events related

265 to El Niño events show a Southwest to Northeast gradient with dry conditions over the NE Amazon region (Malhi et al., 2008), drought events caused by anomalously warm North Atlantic SSTs show a North-South gradient with dry conditions in the southern Amazon region (Lewis et al., 2011; Marengo et al., 2008). Even in the case of El Niño events, SSTs anomalies over the Eastern Pacific (EP) or the Central Pacific (CP) can lead to different impacts and spatial patterns of drought (Jimenez et al., 2019). In addition to their influence on temperature, recent El Niño events also showed amplified atmospheric vapor

270 pressure deficit anomalies (Barkhordarian et al., 2019; Rifai et al., 2019). The impacts of such drought events on humid tropical forests, which are often not adapted to longer-lasting dryness, are severe. Increased forest mortality connected to drought events was observed in central and southern Amazonia (Feldpausch et al., 2016; Lewis et al., 2011; Phillips et al., 2009), as well as shifts in tree species composition (Esquivel-Muelbert et al., 2019). Droughts are assumed to be one of the main drivers for the observed decline in the Amazon carbon sink, indicating that more carbon is lost to the atmosphere than taken up by the

275 forest (Hubau et al., 2020). Thus, such extreme drought events are altering the carbon cycle of the Amazon forest (Feldpausch et al., 2016; Gloor et al., 2015; Hubau et al., 2020; Phillips et al., 2009).

Losing tropical forests in the Amazon region through increased mortality under drought also has implications for regional and continental scale water cycling (Ruiz-Vásquez et al., 2020). The rainforest transpires enormous amounts of water which is transported by winds to remote regions far beyond the borders of the rainforest (e.g. Dirmeyer et al., 2009; van der Ent et al.,

280 2010; Zemp et al., 2014; Zemp et al., 2017). In addition, the ongoing deforestation in the Amazon rainforest further decreases forest cover and thus, transpiration rates, leading to a rainfall decline and enhanced drought conditions in a positive feedback loop (Miralles et al., 2019; Zemp et al., 2017). It can be expected that ongoing climate change most likely will cause stronger and more frequent drought events in the Amazon (Cai et al., 2015; Jia et al., 2019; Marengo & Espinoza, 2016).

For assessing the severity, the spatial extent, and, in particular, the impacts of such drought events on existing ecosystems,

285 different gridded precipitation datasets are available which in some cases differ strongly in magnitude and spatio-temporal distribution of precipitation amounts (Golian et al., 2019). Typical problems of precipitation data for South America encompass the underestimation of extreme rainfall events in both dry or wet seasons (Blacutt et al., 2015; Giles et al., 2020). Therefore, while for the Amazon region, the recent drought events have been assessed in terms of severity (Jiménez-Muñoz et al., 2016;

Jimenez et al., 2018) and impacts (Phillips et al. 2009, Lewis et al. 2011, Feldpausch et al. 2016) based on single precipitation data sets, a systematic analysis of how the most frequent used precipitation datasets differ regarding the spatial extent, location and severity of recent extreme drought events, is currently missing.

For our study, we selected precipitation from nine different datasets: (1, 2) Data from the Tropical Rainfall Measurement Mission (TRMM) version 6 and 7 (Huffman et al., 2007) which have been frequently used, e.g. to estimate drought impacts on the carbon balance (Lewis et al., 2011; Y. Malhi et al., 2009) and are assumed to represent precipitation patterns in the Amazon region best since they are derived from radar measurements (Huffman et al., 2007). (3) CHIRPS (Climate Hazards group Infrared Precipitation with Stations, Espinoza et al., 2019), which has been used to study regional hydro-climatic and environmental changes in the Amazon Basin. These two datasets only provide precipitation and no information about other climatic variables such as temperature or radiation. In addition, we selected five datasets that are often used as drivers for ecosystem models (e.g. in Forkel et al., 2019; Yang et al., 2015) and – in contrast to the other datasets – provide information for more climate variables: Data from the Climate Research Unit (CRU) with a joint project reanalysis (NCEP, National Centers for Environmental Prediction) applied, (4) the CRUNCEP (version 8, Viovy, 2018), (5) the WATCH-WFDEI (WATCH: Water and Global Change, Weedon et al., 2011. WFDEI: WATCH Forcing Data methodology applied to ERA-Interim, Weedon et al., 2014) dataset, originally derived from global sub-daily observations merged with integrations from a general circulation model, (6) the GSWP3 (Global Soil Wetness phase 3, Kim et al. in prep) dataset which is closely related to WATCH-WFDEI, relying on a similar forcing but with a different bias-correction method applied, (7) the newer GLDAS (Global Land Data Assimilation System) 2.1. which is derived from various geostationary infrared satellite measurements and microwave observations (Rodell et al., 2004), (8) the latest ECMWF atmospheric reanalysis dataset, ERA5, which is the successor of ERA-Interim, providing higher spatial and temporal resolutions and a more recent model and data assimilation system than the previous ERA-Interim reanalysis (Albergel et al., 2018), and, finally, (9) the GPCC (named after the Global Precipitation Climatology Centre) dataset (Schneider et al., 2018), which is based on globally available land stations (rain gauges) combined with an empirical interpolation method (Willmott et al., 1985). The data sets were chosen because they are often used to force Dynamic Global Vegetation and hydrological simulation models in climate impacts studies. A more detailed description of the datasets is given in the methods section.

We evaluate the precipitation datasets based on the Maximum Cumulative Water Deficit (MCWD; Aragão et al., 2007), a well-established drought index that is particularly suitable for estimating drought stress in the Amazon region (e.g. Esquivel-Muelbert et al., 2019; Lewis et al., 2011; Malhi et al., 2009; Phillips et al., 2009; Zang et al., 2020). In addition, we included two other measures to complement our analysis: A rainfall anomaly index (RAI), which does account for the mean deviation (in units of standard deviation) of precipitation during the driest months of the year, and the scPDSI (self-calibrating Palmer Drought Index, Wells et al., 2004). The scPDSI index has a more complex formulation compared to RAI and MCWD and takes available soil water content into account. Both RAI and scPDSI have been used in studies describing the recent Amazonian drought events (e.g. Jiménez-Muñoz et al., 2016; Lewis et al., 2011).

The goals of our study are (1) to analyze and quantify the uncertainty in strength, extent, and location of three recent Amazon droughts in the years 2005, 2010, and 2015/2016 in precipitation from nine state-of-the-art precipitation or climate datasets based on MCWD; (2) to examine differences among these drought events by taking two additional drought indicators RAI and scPDSI into account; and (3) to give an estimate of the impacts of the three2005 drought events on the carbon cycle by estimating potential biomass losses.

365

2 Methods

2.1 Study area

Our study covers the Amazon river basin as delineated by ~~Döll & Lehner~~Döll & Lehner (2002, see black contour in Fig. 1). Using 0.5° spatial resolution in longitude and latitude results in 1946 grid cells of interest for this study area. ~~To compare spatial differences of drought extent in more detail, we subdivided the Amazon Basin into 13 regions based on countries and Brazilian states intersecting with the area (SI Fig. 1).~~ Note that differences in the comparison of our results with Lewis et al. (2011) arise because of differences in the delineation of the Amazon region, i.e. the area used in our study is 0.6 ~~Mio~~million km² larger.

2.2 Data sources

~~In the following, we briefly describe the ten precipitation datasets applied in our study (see also Table 1): The Tropical Rainfall Measuring Mission (TRMM v7) product (Huffman et al., 2007) is a precipitation-only dataset based on multiple microwave infrared satellite data developed as a joint product between NASA and the Japan Aerospace Exploration Agency (JAXA). We also included the predecessor v6 for comparison in our study, because it has been frequently and prominently used to derive drought impacts to the Amazon Basin (e.g. Lewis et al., 2011; Phillips et al., 2009) and shows significantly lower precipitation throughout the basin compared to v7 (Seto et al., 2011). Both TRMM datasets are from now on denoted as TR6 and TR7. CHIRPS (Climate Hazards group Infrared Precipitation with Station) is a novel dataset (Funk et al., 2015 from now on denoted CHR) which is a quasi-global (full longitude, but only 50°S – 50°N latitude extent) precipitation-only merged product, based on multi-satellite estimates (similar to TR6 and TR7) and approx. 2,000 in situ observations per month in South America. TR6, TR7 and CHR share the quasi-global spatial extent, however, in comparison to TR6 and TR7 with a resolution of 0.25° x 0.25°, CHR has a much higher spatial resolution of 0.05° x 0.05°. ERA Interim (from now on denoted as ERI) is an atmospheric model that assimilates observation-based estimates from the GPCP dataset (Adler et al., 2003) of the atmosphere during runtime (Dee et al., 2011). Although ERI might show some anomalies in tropical biomes (Di Giuseppe et al., 2013), it has been used for drought evaluation of the Amazon rainforest (Jiménez-Muñoz et al., 2016) and also as a forcing dataset for dynamic vegetation models (DVMs; e.g. Maignan et al., 2011; Poulter et al., 2011). ERA5 (Muñoz Sabater et al., 2018), from now on denoted as ER5, shows improvements in, e.g., land evapotranspiration, surface soil moisture and turbulent heat fluxes over its predecessor ERI (Albergel et al., 2018). Similarly, CRUNCEP (Viovy, 2018 from now on denoted as CRU) is generated based on a reanalysis from the national centers for environmental prediction (NCEP) and the National Center for Atmospheric Research (NCAR), corrected with the CRU TS3.2 (Harris et al., 2014) dataset. GPCC (from now on denoted as GPC) is mainly based on data from rain gauge land stations. Similar to CRU, it is also based on a reanalysis and has been used in global drought studies (Ziese et al., 2014). Both GPC and CRU cover the longest periods of all selected datasets in this study with timespans from 1891 until 2016 and from 1901 until 2016, respectively. WATCH-WFDEI (denoted as WAT from now on; Weedon et al., 2011; 2014) is based on the reanalysis ERI corrected with GPC precipitation. GSWP3 (Kim et al. in prep;~~

4
8

from now on denoted as GSW) is based on the atmospheric reanalysis method "20CR" (20th Century Reanalysis version 2, Compo et al., 2013), which has been dynamically downscaled to 0.5° x 0.5° resolution. Corrections with observational data have not only been applied to precipitation but also to short/longwave radiation, air temperature and the daily temperature range. Both WAT and GSW end in the year 2010. The GLDAS 2.1 (from now on denoted as GLD) dataset is built by using the 'Noah Land surface model' forced by the Goddard Earth Observing System (GEOS) Data Assimilation System with corrected precipitation and radiation (Rodell et al., 2004; Sheffield et al., 2006). Starting in January 2000 (Version 2.1), it is the dataset with the latest time onset and hence defines the lower bound time interval considered in this study. For the 2015/2016 drought event, only seven datasets were available as three of the datasets (TR6, GSW and WAT) end before. All datasets were (if not directly available) converted to 0.5° x 0.5° spatial resolution and to monthly time steps.

2.3. Drought indices and evaluation of drought area and extent

2.3.1 Calculation of maximum climatological water deficit (MCWD)

In the following, we briefly describe the nine precipitation datasets applied in our study (see also Table 1): The Tropical Rainfall Measuring Mission (TRMM v7) product (Huffman et al., 2007) is a precipitation-only dataset based on multiple microwave-infrared satellite data developed as a joint product between NASA and the Japan Aerospace Exploration Agency (JAXA). We also included the predecessor v6 for comparison in our study, because it has been frequently and prominently used to derive drought impacts to the Amazon Basin (e.g. Lewis et al., 2011; Phillips et al., 2009) and shows significantly lower precipitation throughout the basin compared to v7 (Seto et al., 2011). CHIRPS (Climate Hazards group Infrared Precipitation with Station) is a novel dataset (Funk et al., 2015) which is a quasi-global (full longitude, but only 50°S – 50°N latitude extent) precipitation-only merged product, based on multi-satellite estimates (similar to TRMM 6 and TRMM 7) and approx. 2,000 in-situ observations per month in South America. TRMM 6, TRMM 7 and CHIRPS share the quasi-global spatial extent, however, in comparison to TRMM 6, TRMM 7 with a resolution of 0.25° x 0.25°, CHIRPS has a much higher spatial resolution of 0.05° x 0.05°. ERA5 (Muñoz-Sabater et al., 2018) shows improvements in, e.g., land evapotranspiration, surface soil moisture and turbulent heat fluxes over its predecessor ERA-Interim (Albergel et al., 2018), which we decided not to include in our study as it showed higher systematic errors over tropical areas (Nogueira, 2020). Similarly, CRUNCEP (Viovy, 2018) is generated based on a reanalysis from the national centers for environmental prediction (NCEP) and the National Center for Atmospheric Research (NCAR), corrected with the CRU TS3.2 (Harris et al., 2014) dataset. GPCC is mainly based on data from rain-gauge land stations. Similar to CRUNCEP, it is also based on the NCEP reanalysis dataset and has been used in global drought studies (Ziese et al., 2014). Both GPCC and CRUNCEP cover the longest periods of all selected datasets in this study with time spans from 1891 until 2016 and from 1901 until 2016, respectively. WATCH-WFDEI (Weedon et al., 2011; 2014) is based on the reanalysis ERA-Interim corrected with GPCC precipitation. GSWP3 (Kim et al. in prep;) is based on the atmospheric reanalysis method "20CR" (20th Century Reanalysis version 2, Compo et al., 2013), which has been dynamically downscaled to 0.5° x 0.5° resolution. Corrections with observational data have not only been

applied to precipitation but also to short/longwave radiation, air temperature and the daily temperature range. Both WATCH-WFDEI and GSWP end in the year 2010. The GLDAS 2.1 dataset is built by using the 'Noah Land surface model' forced by the Goddard Earth Observing System (GEOS) Data Assimilation System with corrected precipitation and radiation (Rodell et al., 2004; Sheffield et al., 2006). Starting in January 2000 (Version 2.1), it is the dataset with the latest time onset and hence defines the lower-bound time interval considered in this study. For the 2015/2016 drought event, only seven datasets were available as three of the datasets (TRMM 6, GSWP3 and WATCH-WFDEI) end before. All datasets were (if not directly available) aggregated to 0.5° x 0.5° spatial resolution and to monthly time steps.

2.3. Drought indices and evaluation of drought area and extent

2.3.1 Calculation of maximum climatological water deficit (MCWD)

We calculate MCWD based on ~~Aragão et al. (2007)~~Aragão et al. (2007) defining water deficit (WD) as follows:

$$WD(t) = P(t) - ET(t), \tag{1}$$

where $WD(t)$ stands for water deficit, which is calculated for a time step t, in this case for a monthly time step, $P(t)$ for monthly precipitation and $ET(t)$ for monthly evapotranspiration. To estimate the impacts of persistent drought events, the cumulative water deficit (CWD) is defined as the accumulation of water deficit of each month of the hydrological year (see below for details) for which $P(t)$ is smaller than $ET(t)$, ~~hence $WD(t)$ is negative. MCWD is the most negative value of CWD(t) over a specific period. For a complete mathematical definition, see Supporting Information Methods S1. As proposed by Aragão et al. (2007), we use a fixed value for $ET(t) = ET_{fixed} = 100$ mm month^{-1} derived from ground measurements of evapotranspiration in different locations and seasons in Amazonia (von Randow et al., 2004; da Rocha et al., 2004). As a result, water deficit builds up whenever the~~ hence $WD(t)$ is negative. MCWD is the most negative value of CWD(t) over a specific period. As proposed by Aragão et al. (2007), we use a fixed value for $ET(t) = ET_{fixed} = 100$ mm month^{-1} derived from ground measurements of evapotranspiration in different locations and seasons in Amazonia (da Rocha et al., 2004; von Randow et al., 2004). As a result, water deficit builds up whenever monthly rainfall $P(t)$ falls below 100 mm.

We calculate annual MCWD for the hydrological year from October of the previous year to September of the succeeding year, e.g. the MCWD for the year ~~2000~~2005 is calculated from October ~~1999~~2004 to September ~~2000~~2005 (similar to Lewis et al., 2011). ~~Similarly, for deriving~~

In contrast to e.g. Lewis et al. 2011, we use the ~~drought severity, we calculated the~~relative MCWD anomaly (~~ΔMCWD)~~from now also denoted as rMCWD) as our main drought indicator. For deriving rMCWD, we estimate the absolute MCWD anomaly (from now also denoted as aMCWD) for 2005 and 2010, respectively, by first calculating the mean MCWD for the "baseline" period from 2000 to 2010~~, thereby excluding the years~~ and second by subtracting the mean MCWD from 2005 and 2010~~. To derive ΔMCWD, the baseline period is subtracted from the mean value of 2005 and 2010, respectively.~~, respectively. The rMCWD anomaly is then estimated as the normalized deviation of the aMCWD anomaly in units of standard deviation. The same procedure was applied for ~~calculating ΔMCWD~~the rMCWD anomaly for 2016, extending the baseline period ~~to~~

from 2000 to 2016 and additionally excluding the year 2016. We excluded the drought years from the baseline period as the high proportion of drought years would bias the mean water stress (Lewis et al., 2011). We investigated also the effect of including drought years in the baseline calculation and the role of a longer baseline period (Fig. S1). Similar to Lewis et al. 2011, we defined ΔMCWD from 2000 to 2016.

We define relative thresholds of rMCWD anomaly < -0.5 as moderate, rMCWD anomaly < -2.0 as severe, and rMCWD< -2.5 as extreme drought stress. Previously, levels of drought stress were based on aMCWD anomaly (often also referred to as ΔMCWD, e.g. Lewis et al. 2011) with aMCWD anomaly < -25 mm as moderate drought stress because at this level, tree mortality already significantly increased in their inventory plots. We further defined ΔMCWD < −100

By comparing empirical cumulative density functions of aMCWD and rMCWD anomalies (Fig. S1 and Methods S1) we are also able to give absolute estimates for our relative thresholds with aMCWD < -26 mm as severe and ΔMCWD < −150, aMCWD< -106 mm as extreme drought stress, and aMCWD < -132 mm reflecting moderate, severe and extreme drought stress, respectively. Choosing relative anomalies over absolute enables a direct comparison of MCWD to the other drought indices used in this study. We used the rMCWD anomaly for the majority of the analysis conducted in our study except for the impact of drought on aboveground biomass (section 2.4 and Fig. 4), where we use the aMCWD anomaly. We also estimated seasonal patterns of cumulative water deficit (CWD), by defining rCWD similar tor rMCWD as the relative anomaly of each month's CWD in units of standard deviation.

2.3.2. Calculation of rainfall anomaly index (RAI)

For the rainfall anomaly index, dry season rainfall was taken as the mean precipitation from July-September following Lewis et al. (2011). For each year, the 'standardized anomaly' was calculated as the anomaly of rainfall expressed as the difference in units of standard deviation from the Like for the MCWD estimation, we calculated the mean dry season rainfall over all years. Like for to the MCWD calculation, we excluded the drought years 2005 and 2010 from the mean dry season precipitation calculation from a baseline period 2000-2010 to investigate the drought impacts of 2005 and 2010, and for 2016 we selected a baseline period from 2000 to 2016 excluding 2005, 2010, and 2016. We defined RAI < −1 to represent moderate, RAI < −2 to represent severe, and RAI < −3 to represent extreme drought stress. The relative rainfall anomaly index (rRAI) was estimated as 'standardized anomaly' from the baseline period similarly to the rMCWD anomaly calculation. As rRAI only reflects the precipitation anomaly during July and September, it can also be described as a dry season anomaly.

2.3.3. Calculation of the self-calibrating Palmer Drought Severity Index (scPDSI)

The self calibrating Palmer Drought Severity Index (scPDSI, Wells et al., 2004) has in recent studies been used to assess the impacts of droughts on the Amazon basin (e.g. Jiménez Muñoz et al., 2016). It improves the original PDSI by using a self calibrating procedure based on historical climate data, eliminating the empirically derived climatic characteristics. Next to precipitation, it also takes monthly potential evapotranspiration ET into account. In our study, we use ET data generated by

the ER5 reanalysis. Additionally, the scPDSI takes soil water capacity as input, which we assumed here as a constant value of 100 mm. scPDSI was estimated using the *R* package *scPDSI* (Ruida et al., 2018).

To enable comparison with the MCWD and RAI, we selected identical baseline periods from 2000 to 2010 for the 2005 and 2010 events and from 2000 to 2016 for the 2016 drought event. We also adopted the categorization from Jiménez-Muñoz et al. (2016) and Wells et al. (2004) with *scPDSI* < −2 representing moderate, *scPDSI* < −3 severe and *scPDSI* < −4 extreme drought stress.

The self-calibrating Palmer Drought Severity Index (scPDSI, Wells et al., 2004) has in recent studies been used to assess the impacts of droughts on the Amazon basin (e.g. Jiménez-Muñoz et al., 2016). It improves the original PDSI by using a self-calibrating procedure based on historical climate data, eliminating the empirically derived climatic characteristics. Next to precipitation, it also takes monthly potential evapotranspiration ET into account. In our study, we use ET data generated by the ERA5 reanalysis. Additionally, the scPDSI takes soil water capacity as input, which we assumed here as a constant value of 100 mm. scPDSI was estimated using the *R* package *scPDSI* (Ruida et al., 2018).

To enable cross-comparison with the rMCWD and rRAI anomalies, we selected identical baseline periods from 2000 to 2010 for the 2005 and 2010 events, and from 2000 to 2016 for the 2016 drought event. Again, we used the relative deviation $r$scPDSI, defined as 'standardized anomaly' from the baseline period of monthly scPDSI values as drought indicator.

2.3. Calculation of drought area and extent

Each grid cell's area was approximated as a trapezoid to its boundary coordinates (in 0.5° x 0.5° resolution), resulting in an area between 2900 and 3090 km² per grid cell. Accumulating the associated areas over all grid cells resulted in a total area of 5.94 million km² representing the Amazon Basin. Note that for comparison of our results with Lewis et al. (2011) differences in absolute areas arise because of differences in study area size (5.94 vs. 5.3 million km², respectively). For the calculation of the drought-affected area, we summed up the area of grid cells that matched the respective drought classification (e.g. AMCWD < −150 mm rMCWD anomaly < −2.5 for extreme drought stress). The spatial agreement of drought location among datasets was estimated by selecting the grid cells matching the drought classification per dataset and subsequently counting the number of datasets per grid cells showing the respective drought classification.

2.4. Estimating carbon losses during drought events

To estimate carbon loss during drought events, we used a simple linear relation between MCWD and$a$MCWD anomaly and aAGB, the change in aboveground biomass, i.e. biomass carbon losses in the Amazon basin derived from plot measurements (Lewis et al., 2011):

~~ΔAGB~~ *a*AGB= 0.3778 - 0.052 * ~~ΔMCWD~~*a*MCWD

(2)

700

~~Here, ΔAGB denotes the change in aboveground biomass, i.e. biomass carbon losses.~~ The equation was derived from Amazon plot inventory data measured across the RAINFOR network to estimate the impact of the 2005 drought event (Lewis et al. 2011). To calculate ~~ΔAGB~~the *a*AGB anomaly in Eq. 2, we ~~used~~calculated the ~~ΔMCWD~~*a*MCWD anomaly of each gridcell ~~for each drought year calculated~~ in 2005 for each of the precipitation datasets in our study. The total biomass carbon loss (in 705 ~~Pg C~~PgC) across the Amazon basin is then calculated by summing up ~~ΔAGB~~*a*AGB anomaly for all gridcells weighted by each gridcell's size.

3. Results

All areas in the following section are expressed as percentage ~~with respect to~~of the entire Amazon basin according to our delineation (5.94 million km²). For an overview of the areas affected in million km², see Table ~~2~~S2 and ~~3~~S3.

3.1 Comparison of total drought area based on ~~AMCDW~~relative MCWD anomaly

745 We first evaluate differences in ~~the two TRMM products, TR6 and TR7. For 2005 and 2010, we find similar spatial patterns~~ rMCWD for ~~TR7, as in Lewis et al. 2011 for TR6~~2016 across the datasets (Fig. ~~1a, b). Regarding drought intensities, TR7 agrees with its predecessor TR6 for 2005, showing a slightly smaller area (4% less), but an 11% smaller area for 2010. AMCWD calculated from TR7 indicates~~1). Here, we find that the ~~North-Western region~~spatial patterns of the rMCWD anomaly generally match across~~Amazon Basin (particularly~~ the ~~Roraima region) was hit extremely by~~available datasets,
750 showing severe and extreme drought stress mainly in ~~2016 with 7% of~~ the ~~area having AMCWD < −150mm (Fig. 1c).~~ ~~Furthermore, in 2016 about 15% of the~~ northern Amazon basin~~was severely affected by~~. Only GLDAS diverges, showing extreme drought stress ~~located at~~in the Central and Western part ~~and scattered in South Eastern~~ of Amazonia. ~~Moderate~~ (Fig. 1d) where none of the other datasets show any drought stress ~~was found throughout 54%~~during the same year. The other datasets mostly differ regarding the intensity of the drought stress. While ERA5 and TRMM7 show values rMCWD < -2.5 in
755 the Columbian part of the basin~~also affecting central~~, CRUNCEP and ~~western Amazonia (Fig 1c).~~GPCC do show such a strong drought impact only in Northern Brazil. The absolute areas of drought stress across different severity levels are similar across most datasets with only GLDAS showing a significantly larger area affected by extreme drought stress of rMCWD < -2.5.

760 Across all precipitation datasets, in 2005, an area ranging from ~~46~~37 to ~~71~~51% (mean ~~53~~45%) of the whole Amazon basin, was moderately affected (Table ~~2~~S2, Fig. 2a). ~~GSW and GLD~~ERA5 displayed the smallest area affected by moderate drought (2.~~6~~2 million km², Tab. 1, Fig. 2), while ~~ER5~~CHIRPS and CRUNCEP showed a vast affected area (4.~~2~~3.0 million km²), an area about ~~12~~36% larger than displayed by ~~ERI~~ERA5. For severe and extreme drought conditions, ~~CHR~~ERA5 shows the smallest affected area with ~~6~~3% and 1% of the basin ~~and no~~ affected ~~area, respectively.~~. For severe drought conditions,
765 ~~CRU~~CRUNCEP suggests that an area approximately ~~16% more of the basin area~~3 times larger was affected ~~in comparison~~compared to ~~CHR (1~~ERA5 (0.2 million km² vs. 0.6 million km²~~vs. 0.4 million km²~~). ~~CRU~~CRUNCEP and GLDAS also ~~encompasses~~encompass the largest area of extreme drought stress (0.~~7~~2 million km²; ~~12~~3% of the basin less than ~~AMCWD < −150mm).~~ rMCWD < −2.5, Fig. 2a).

During the 2010 drought, a larger area ~~was affected by moderate drought~~ ranging between a minimum of 52% (~~GPC~~GPCC)
770 and a maximum of ~~76% (TR6),~~74% (TRMM 6) was affected by moderate drought stress, which is about ~~10~~36% larger than during the 2005 drought (3.~~1~~6 million km² vs. 4.~~6~~2.7 million km², ~~Tab. 2~~Table S2, Fig. 2). In addition, the area ~~with~~under severe drought ~~extent~~stress was on average ~~3~~25% larger compared to 2005. ~~The~~ and the area affected by extreme drought was

~~4~~
14

smaller than during~~double~~ the size of the 2005 drought event. Particularly, ~~ER5~~GLDAS and ~~TR6~~TRMM 6 showed the largest area affected throughout the three drought classifications (Fig. 2b).

805

For 2016, two datasets (~~CHR~~CHIRPS and ~~CRU~~CRUNCEP) showed with 4038% a considerably smaller area that was moderately affected by drought stress compared to ~~ER5 and ERI~~GLDAS with ~~69% and~~ 63% of the area affected, respectively (datasets ranging between 2.42 and 4.13.7 million km²). Generally, in 2016, the size of the area affected by moderate drought was in between the size of the area affected in 2005 and 2010, but the extent of severely and extremely drought-affected areas was larger. Here, particularly ~~ERI (closely~~GLDAS followed by ~~ER5)~~GPCC showed the largest affected area, with 3021%

810 severely affected and 186% extremely affected. (Table S3).

3.2 Spatial agreement of rainfall datasets using ~~AMCDW~~the *r*MCDW anomaly

While the agreement of the total area affected by drought is relatively high (see 3.1~~),~~) the data sets ~~are~~ only partly ~~in agreement regarding~~agree on the spatial ~~patterns~~extent and ~~locations~~location of ~~the 2005,~~ extreme drought conditions, particularly during

815 the 2010 and 2016 ~~droughts~~events (Fig. 3). For 2005, all datasets ~~are in agreement regarding~~agree on the drought epicenter being located in Central Amazonia ~~mainly affecting the Brazilian states~~ *Amazonas and Acre* (Fig. S4 b, d). All ten datasets also. Datasets agree that an area of about 15 % of the Amazon Basin was at least moderately affected (Fig. 3a). Only a small overlap was found for the area affected by severe and extreme drought stress (Fig. 3b, c). Here, only half of the datasets agreed on 114% of central Amazonia being severely and 41.5% extremely affected.

820 For 2010, all datasets agreed on an affected area of 1121% in the Amazon basin, and half of the datasets agreed on an area of 7260% of the Amazon Basin being moderately affected by drought stress (Fig. 3d). The 2010 drought displayed no central hotspot, but three most affected areas in the Eastern, Southern and central ~~part~~parts of Amazonia on which most of the datasets agreed (Fig. 3d). Severe drought stress in 2010 was located in the southern part of Amazonia, where four datasets agreed (Fig. 3e), while for extreme drought stress almost no overlap between datasets was found (Fig. 3f).

825 For 2016, all datasets agreed on an area of about ~~8% for~~7% of moderate drought stress and half of the datasets agreed on 5451% of the basin being affected (Fig. 3g). Agreement for severe and extreme drought stress was ~~higher~~lower compared to the other drought years (Fig. 3h, i). Most of the ~~data sets~~datasets located the epicenter of the drought in the ~~North-Western part of Amazonia~~north-western Amazon basin. Some datasets also showed the South-Central part of the basin being severely affected (Fig 3i).

830 ### 3.3 Estimating the variation of carbon losses during drought events

For the different precipitation datasets and based on the linear relation between ~~AMCWD~~*a*MCWD and ~~AAGB~~*a*AGB anomaly, we derive carbon losses for 2005 to be in the range of 0.7-1.3 ~~1.9 Pg C~~6 PgC with ~~CHR~~ERA5 showing the smallest and

4

15

865 ~~CRU~~CRUNCEP the strongest impact regarding carbon losses (Fig. 4). The mean biomass loss ~~over all~~overall datasets was 1.~~6 Pg C~~2 PgC with ~~six~~five of the ~~ten estimates from the different datasets~~ nine estimated carbon losses being close to that mean (difference of ~~ΔAGB~~aAGB anomaly less than 0.~~15~~1 PgC to the mean value). ~~For 2010, carbon losses range from 1.5 to 2.3 Pg C with WAT showing the smallest and TR6 strongest response. Next TR6 also ER5 shows a very strong drought impact with 2.3 PgC. All other datasets show much smaller impacts~~Because no relationship between ~~1.6 and 1.8 Pg C comparable to~~

870 ~~the 2005 drought impact. The 2016 drought event shows the widest range~~the anomalies of ~~biomass loss across datasets ranging from 1.3 PgC to 2.5 PgC. The disagreement between datasets is also larger~~ aMCWD and aAGB could be verified for ~~2016 compared to 2005 and 2010: Both, CRU and CHR show a low impact of 1.3 Pg C, TR7 and GPC show 1.7 Pg C biomass loss comparable to the averages of 2005 and 2010. GLD, ER5, and ERI show very strong impacts of 2.1, 2.3 and 2.6 Pg C, respectively.~~ 2010 (Feldpausch et al., 2016) we did not estimate the impacts on AGB for the other drought years 2010 and

875 2016.

3.4 Comparison of drought indices: ~~ΔMCDW, scPDSI~~rMCDW, rscPDSI and ~~RAI~~rRAI anomalies

Similar to ~~ΔMCWD~~rMCWD, there is variable agreement among datasets when evaluating the other two drought metrics, ~~RAI~~rRAI and rscPDSI (Fig. ~~5). scPDSI showed the lowest agreement across datasets, with mainly two datasets in agreement on areas affected by drought for 2005. Regarding the total area affected in 2005, TR7 showed the~~5). The largest ~~area (48% of

880 the Amazon basin, 2.8 million km²) and GLD (32%, 1.9 million km², Table 2) the smallest area affected by drought stress. Severe drought stressed areas ranged between 16% (GLD) and 26% (CRU) and extreme drought stress between 1% (GLD) and 5% (CRU) of the basin affected. The largest rainfall anomaly (RAI) for moderate drought stress~~dry season anomaly (rRAI) in 2005 was displayed by ~~CHR~~GPCC with ~~52% (3.1~~6.5% (0.4 million km², Table ~~2~~S2), followed by ~~ER5~~TRMM 7 with ~~49~~5.7% of the ~~area~~Amazon basin being severely affected. ~~CRU~~ERA 5 showed with ~~29~~3% the smallest area affected ~~by drought stress.~~

885 ~~The area of~~ . In 2005, spatial patterns of rRAI matched with rMCWD anomalies despite rMCWD anomalies showing a larger area affected by severe drought stress ~~was smaller using RAI compared to~~ (Fig. 5a, d). rscPDSI~~, ranging from 9 to 20%. In general, the datasets~~ displayed ~~a more spatially connected~~the smallest area affected by drought stress in ~~the center of the Amazon basin when using RAI compared to scPDSI. RAI~~2005 with also only GPCC and ~~MCWD agreed on the spatial location of the drought, while scPDSI~~TRMM 7 showing with 5.5% and 3.1% the largest severely affected area, respectively. All other

890 datasets showed less than 1% of severe drought ~~stress~~affected areas in ~~a different region~~2005. The small spatial area of rscPDSI differed compared to the other two drought indicators (Fig 5a, d, g): Some areas showed a strong disagreement between drought indices, e.g. ~~a small area in Western Brazil and Peru~~Central Amazonia was hit by severe drought stress according to ~~ΔMCWD~~rMCWD and ~~RAI~~rRAI (with ~~all~~3-4 climate datasets in agreement~~). In~~) while, in contrast, ~~scPDSI~~rscPDSI did not indicate abnormally dry conditions there.

895 ~~In 2010, the total droughted area was similar for scPDSI and smaller for RAI compared to MCWD regarding severe drought stress (Fig. 5b, e, h): For scPDSI, in particular, GLD showed a large area of 50% of the basin severely affected (2.9 million~~

4

16

ForIn 2010, the differences of drought-affected areas were even more pronounced between the three indices (Fig. 5b, e, h). Here, ERA5 and TRMM7 showed the largest areas affected by severe drought stress based on the dry season rRAI anomaly with 7% and 5%, respectively. Using $r$scPDSI all datasets showed an area between 1% and 2.5% severely affected. Interestingly, the area affected based on rMCWD roughly encompasses the area affected by rRAI, but additionally shows a large area in the South-Eastern part of the basin being affected by severe drought stress (Fig. 5b, e).

In 2016, $r$scPDSI showedshows the largest area affected by drought stress with GLDGLDAS showing 6239% (followed by TR7, 52TRMM7, 16%) of the basin being severely affected. Four datasets agreed on the affected area in the northeastern part of the basin (Fig. 5f). Hardly any5i). Only one dataset (GLDAS) showed severe drought stress was visible in 2016 when calculating dry season rainfall anomalies (RAIrRAI , Fig 5i5c), indicating no pronounced anomalies in dry season rainfall. Only GLD diverted from the other datasets showing 30% of the area under severe drought stress, while according to all other datasets found between 0-1% of the area to be affected (Table 3). ΔMCWD. rMCWD and scPDSI again$r$scPDSI roughly agreed on the spatial extent of the droughted area (Fig. 5c, f). Generally, scPDSI showed a much larger areanorthern part of the basin being severely affected by drought stress over ΔMCWD and RAI.(Fig. 5f, i).

SeasonalAverage seasonal patterns of median ΔMCWD across the Amazon basin wereare quite consistent for 2005, where all across datasets showed a sudden but differ depending on the choice of drought impact (decline in ΔMCWD) from July onwards. Only ERIindex and ER5 displayed a small decline already in the months before July. drought event (Fig. 6). The strongest (most negative) rainfall anomaly was visible from May to July during the 2005 drought event (Fig. 6a). Accumulating such low rainfall estimates resulted in very low values of rCWD during that period (Fig. 6d) in 2005. $r$scPDSI values were also low, but more constant throughout the year (Fig. 6g).

The 2010 drought followed similar patterns regarding ΔMCWD,rRAI with a lower absolute impact during May to July compared to 2005 (Fig 6b). For 2015, datasets agreed on a small decline in ΔMCWD followed by a more substantial impact in 2016 with fewer datasets in agreement (Fig Interestingly, the wet season months March to May showed a strong anomaly during 2010 compared to the 2005 event. Subsequently, rCWD was also already lower during the wet season in 2010 compared

965 to 2005 (Fig. 6e). $r$scPDSI anomalies values were similar for 2010 compared to 2005 with a slightly downward trend towards the end of the year (Fig. 6g, h).

To investigate 6e). Datasets agreed well according to the seasonal patterns of scPDSI for 2005 and 2010 (Fig 6d, e). This agreement was lower for the year 2016, in which CRU, GLD and TR7 indicate drought stress already starting in January, and ERI and ER5 only starting in September (Fig. 2016 we also considered6f). All datasets showed a period of drought stress for

970 longer than 12 months. Datasets generally agreed on rainfall anomaly (RAI) patterns for all of the drought indices of 2015 since both years were El Niño years. We found a strong rainfall anomaly already starting during September 2005, 2010, and 2016 (Fig. 6g, h, i). For 2005 the difference in rainfall was highest in June-July and for 2010 in March, August and September. The 2015 continuing until April 2016 (Fig. 6c). /2016 drought event showed a longConsequently, also rCWD values were very low during that period (Fig. 6f). of strong (negative) rainfall anomaly While rMCWD was applied as the maximum value

975 from AugustOctober to September, drought stress before October of the previous year cannot be accounted for when using rMCWD. The two-year drought impact was also visible using scPDSI (Fig. 6i) showing a steady decline from 2015 to July 2016 (Fig. 6i).

4. Discussion

We assessed the severity and spatial extent of the extreme drought years 2005, 2010, and 2015/2016 in the Amazon region ~~and their impacts on the carbon cycle.~~by computing different drought indices using a range of precipitation datasets. When analyzing how drought ~~representation~~conditions are captured in ~~ten~~nine different precipitation datasets for the Amazon basin, we find that while the datasets mostly agree on the extent of the drought area, they differ in their location of drought. ~~We show that~~We found a wide range between 0.7 and 1.7 PgC of potential biomass losses during 2005 ~~and 2010 were~~with most datasets showing an impact of about 1.~~8 PgC, indicating that the more intense drought in 2005 equals a larger total area of the 2010 drought regarding biomass loss. In 2015/2016, we find a large variability of biomass losses depending on the precipitation dataset used, ranging from 1.3 to~~2.7 PgC.

Critical aspects regarding the detection of drought events in the Amazon basin

Drought indices

The idea of defining water deficit based on evapotranspiration rates goes back to Stephenson (1998) and the MCWD is now one of the most widely used ~~measures~~indicators to assess drought stress in tropical forests (e.g. Lewis et al., 2011, Phillips et al., 2009, Esquivel-Muelbert et al., 2019). ~~The~~In its simplest form, the calculation of MCWD only requires precipitation data and assumes a constant evapotranspiration (ET) rate of 100 mm month^{-1} ~~(Aragão et al., 2007). Although the simplicity of AMCWD~~(Aragão et al., 2007). Although the simplicity of rMCWD and aMCWD is a main advantage, a fixed ET (which we also used in our study) is inappropriate for regions other than the lowland tropics, where the lower supply of energy may result in lower ET values. Most importantly, an approximated ET does not account for either seasonal variation (driven mainly by radiation, temperature, and phenology) or spatial variation in ET related to soil and root properties (Malhi et al., 2009). Hence, changes in ~~AMCWD~~rMCWD are purely accounting for changes in rainfall (Phillips et al., 2009). In contrast, scPDSI is driven with spatially and temporally resolved evapotranspiration data (here: ~~ER5~~ERA5). However, currently available evapotranspiration products for the Amazon rainforest show significant differences in areas and extent of evapotranspiration ~~(Sörensson and Ruscica, 2018), hence introducing another source of uncertainty when using it for the calculation of drought indices.~~ (Sörensson & Ruscica, 2018), hence introducing another source of uncertainty when using them for the calculation of drought indices. In the last decade, better products of spatially and temporally resolved evapotranspiration data (e.g. ERA5) have been developed and an increasing number of studies are now estimating MCWD based on such data (e.g. Staal et al., 2020). However, using a constant evapotranspiration (ET) rate of 100 mm month^{-1} across the Amazon rainforest is still very common (e.g. Flack-Prain et al., 2019; Koch et al., 2021).

We investigated the effect of choosing variable evapotranspiration and a longer baseline in our MCWD calculation (Fig. S3). Using variable evapotranspiration consistently reduced the moderate drought-affected area by 10-20% per drought event (Fig. S3a, b, c). It also affected the intensity of the drought stress, e.g. areas previously classified as extreme drought stress were now classified as areas under severe drought stress. This reduction is expected as ERA5 takes the above-mentioned lower ET

values in the highland tropics into account which overall leads to higher MCWD values in this region. Because of the strength and consistency of this effect we recommend testing the MCWD calculation regarding its sensitivity to variable ET in the tropical rainforest in future studies. In contrast, extending the baseline period of the MCWD calculation to include also years before 2001 leads to overall lower MCWD values and, hence, an increased intensity of the three drought events (Fig. S3d, e, f). This finding highlights the drought anomaly that the recent decade from 2001 to 2016 has compared to the years before that period.

The key difference between the three drought indices applied in our study is the temporal resolution: RAI is only calculated for the three driest months (July-September) and thus, for example, a rainy season with deficient rainfall is not captured. ~~ΔMCWD, in contrast, accumulates over 12 months and is reset to zero at the end of the hydrological year. In this way, drought events caused by low precipitation in both dry- and rainy season are captured, however, drought events lasting for longer than a year are not detected. scPDSI is not reset to zero at the end of the hydrological year and is thus captures also multi-year drought events. As an example, the 2015/2016 drought event is classified as a severe multi-year drought according to Yang et al. (2018), which is also displayed in our analysis when using scPDSI (all datasets in agreement that more than 30% of the area were affected, Tab. 3). ΔMCWD and RAI, however, do not agree on a spatially and temporally extensive drought event (Fig. 5c, f, g, Tab. 3), but instead display distinct regions of severe drought stress. Thus, this drought event seemed not to be characterized by particularly low dry season precipitation, but by low precipitation accumulated over a longer time period. scPDSI and ΔMCWD roughly agreed on spatial extent but scPDSI showed a more substantial drought impact indicating that precipitation levels might have been already lower than usual during the years before the 2016 drought event happened, indicating a multi-year drought event (Yang et al., 2018).~~ MCWD, in contrast, accumulates over 12 months and is reset to zero at the end of the hydrological year. In this way, drought events caused by low precipitation in both dry- and rainy seasons are captured, however, drought events lasting for more than a year are not detected. scPDSI captures multi-year drought events and is not reset to zero at the end of the hydrological year. ~~Seasonal patterns of the three drought indices support this assumption (Fig. 6): Resetting MCWD once per year neglects any influences of drought events of the preceding year (Fig. 6c).~~

These differences between the drought indicators can be seen for the three drought events analysed in this study. In 2005, rRAI and rMCWD values roughly match in location of the epicenter indicating a particularly strong anomaly during the dry season (Fig. 5a, d). This does not apply to the 2010 drought event, where despite some dry season anomaly an even stronger anomaly during the wet season is visible (Fig. 6b, e). The 2015/2016 drought event is classified as a severe multi-year drought according to Yang et al. (2018), which is also displayed in our analysis when using $r$scPDSI, (Fig 6i). rMCWD and rRAI, however, do not agree on a spatially and temporally extensive drought event in 2016 (Fig. 5c, f, i), but instead display distinct regions of severe drought stress. Seasonal patterns of the three drought indices support this assumption (Fig. ~~A common drawback of all drought metrics used in our study is their incapability to explicitly represent the effect of increasing atmospheric vapor pressure deficit (VPD) on plant water stress. A steady amplification of atmospheric vapor pressure deficit~~

4
20

Precipitation datasets

6): Resetting rMCWD once per year neglects any influences of drought events of the preceding year (Fig. 6c). While the drought indices used in this study showed pronounced differences in spatial and temporal dynamics, including all of them can help better understanding the different characteristics that drought events can have in the Amazon basin.

A common drawback of all drought metrics used in our study is their incapability to explicitly represent the effect of increasing atmospheric vapor pressure deficit (VPD) on plant water stress. A steady amplification of atmospheric vapor pressure deficit (VPD) has been detected over the Amazon basin (Barkhordarian et al., 2019; Rifai et al., 2019). Such stronger atmospheric water demand leads to additional water loss of plants during drought, subsequently increasing the severity of droughts. Hence, the role of VPD during a drought and as a driver for plant stress should not be underestimated (Grossiord et al., 2020). With increasing data availability and better estimates of VPD across the Amazon region, it should be included in future drought assessments (e.g. Castro et al., 2020). One possibility to account for the influences of VPD is choosing temporal and spatially resolved evapotranspiration instead of constant evapotranspiration in the calculation of MCWD. Future studies could further investigate the relationships between MCWD, ET, and VPD and the impacts on biomass.

Furthermore, in the last decade, new methods have been developed that assess impacts of drought on ecosystems, e.g. analyses based on solar-induced fluorescence (SIF) data show that tall forests are less sensitive to rainfall compared to short forests (Giardina et al., 2018). Also, vegetation optical depth (VOD) used as a proxy for water content in forests is a promising satellite-derived indicator for mortality and impacts of droughts on forests (Rao et al., 2019). However, conducting analyses over the Amazon rainforest based on VOD is difficult, because of the limited penetration depth of microwaves in dense tropical forests (Chaparro et al. 2019), and the influences of vegetation water status (Xu et al. 2021). So far, VOD data could only be

1210 applied with limited success across tropical rainforests (Konings & Gentine, 2017). Future studies should estimate the impacts of droughts based on multiple drought characteristics. For example, Toomey et al. (2011) show that considering both, heat stress and soil moisture stress greatly improves the explanatory power of drought impacts in the Amazon basin.

Precipitation datasets

1215 For the three drought events in 2005, 2010 and 2016, ~~ERI~~CHIRPS, GLDAS and ~~ER5~~ERA5 diverted the most from the other datasets regarding the ~~size of the area affected by drought. Especially ER5 shows~~spatial drought extent. ERA5 shows the smallest area of moderate drought stress during 2005 but one of the largest ~~area of moderate drought stress during all three drought events (Fig. 2). Although TR7 and CHR~~areas in 2010 (Fig. 2). We found no obvious bias between the precipitation datasets regarding distribution and frequency of monthly rainfall (Fig. S2) with only ERA5 showing higher rainfall more

1220 frequently. Although TRMM7 and CHIRPS are based on the same satellite data as ~~the~~their input, they differ regarding the size of the drought area, especially during 2016 (Fig. 2). Lewis et al. (2011) estimated an area of 47% (2.5 million km²) of the Amazon basin moderately affected in 2005 using the ~~TR6~~TRMM6 dataset, which compares well with the size of the affected area ~~in~~for the ~~GLD, GPC, and GSW~~majority of datasets ~~analysed~~analyzed in our study (considering our 0.6 million km² larger study area; see Methods). For 2010, Lewis et al. (2011) reported an area of 3.2 million km² being affected in comparison to

1225 4.5 million km² in our analysis using ~~TR6~~TRMM6 with very similar spatial patterns. The newer ~~TRMM~~ product, ~~TR7~~TRMM7, however, shows less frequent rainfall but heavier rainfall than ~~CHR~~CHIRPS maintaining a similar total amount ~~(Giles et al., 2020).~~of precipitation (Giles et al., 2020). Also, both ~~TRMM~~ versions (~~TR6~~TRMM6 and ~~TR7~~TRMM7) differ regarding the total area affected by drought stress in 2005 and in particular in 2010 ~~with TR6 showing~~, where TRMM6 showed a ~~14~~10% larger area of the Amazon basin affected ~~in our analysis.~~. This can be explained by the generally higher precipitation rates

1230 detected in the ~~TR7~~TRMM7 dataset in comparison to ~~TR6 (Seto et al., 2011)~~TRMM6 (Seto et al., 2011) leading to lower absolute values of ~~A~~MCWD*r*MCWD. Spatially, this difference was most pronounced in the western and northern parts of Amazonia, in the *Acre* and *Roraima* states, and in Peru. Because of such higher precipitation rates in ~~TR7~~TRMM7 as compared to ~~TR6~~TRMM6, and subsequently the much stronger drought response according to our analysis, studies ~~only~~ based on ~~TR6~~TRMM6 only might overstate the actual drought conditions and should be revisited. Precipitation datasets usually show

1235 remarkable differences in the representation of occurrence, frequency, intensity and location of events, mainly due to their nature of high spatial and temporal variability ~~(Covey et al., 2016; Dirmeyer et al., 2012).~~(Covey et al., 2016; Dirmeyer et al., 2012). Generally, the sparse network of observations in the Amazon rainforest may explain the differences across precipitation datasets and drought indices for datasets that rely on station data. Within the last decade, the number of observations increased, due to a new denser network of stations. This may improve the reanalysis models that are used for several precipitation datasets

1240 applied here, however, it does not improve datasets that only rely on gauge observations.

~~According to Jiménez Muñoz et al. (2016), 40%, 25% and 10% of the Amazon basin were affected by moderate, severe and extreme drought stress in March 2016 when using scPDSI, respectively. This is similar to our estimate (46%, 34% and 9%,~~

moderately, severely and extremely affected in Sep 2016) based on the same precipitation dataset (ERI). Our estimate slightly diverted from the results of Jiménez-Muñoz et al. (2016), again at least partly due to a different reference area (see Methods). In addition, they used spatially resolved information on soil water capacity when calculating scPDSI and a longer baseline period (start year is 1979 in their study vs. 2000 in our study). scPDSI generally seems to be more sensitive to baseline changes (Fig S2e). In addition, also the choice of the precipitation dataset plays an important role. In regions, in which ER5 showed an extremely affected area of only 5%, other datasets such as GLD and TR7 showed a much stronger drought impact with over 70% of the area moderately and between 50% and 60% severely affected. This is particularly interesting because recent studies identify TR7, CHR and ER5 as best precipitation datasets when comparing to gauge observations in South America (Albergel et al., 2018; Burton et al., 2018; Rifai et al., 2019). The higher variability that scPDSI showed across datasets can be explained with the more complex algorithm (including the self-calibrating mechanism) compared to MCWD and RAI.

Jiménez-Muñoz et al. (2016) quantified drought extend using the scPDSI and found that 40%, 25% and 10% of the Amazon basin were affected by moderate, severe, and extreme drought stress, respectively, in March 2016. While we did not evaluate scPDSI directly but focused on $r$scPDSI to allow for a better cross-comparison to the other drought indicators, we found similar patterns for moderate drought stress (47% of the basin affected), but different patterns under severe (11%) and extreme (1%) drought stress when evaluating $r$scPDSI using the ERA5 dataset. Our estimation diverted from the results of Jiménez-Muñoz et al. (2016) mainly because of our different drought classification, but also due to a different reference area (see Methods).

In addition, Jiménez-Muñoz et al. (2016) used spatially resolved information on soil water capacity when calculating scPDSI and a longer baseline period (year onset is 1979 in their study vs. 2000 in our study). Furthermore, the choice of the precipitation dataset plays an important role. Compared to the datasets considered in our study, ERA 5 showed the weakest drought impact during the 2016 drought event. GLDAS and TRMM7 showed a much stronger drought impact with over 70% of the area moderately and between 15% and 39% severely affected (Table S3). This is particularly interesting because recent studies identify TRMM7, CHIRPS and ERA5 as the best precipitation datasets when comparing to gauge observations in South America (Albergel et al., 2018; Burton et al., 2018; Rifai et al., 2019). The higher scPDSI variability across the precipitation datasets can be explained with the more complex algorithm (including the self-calibrating mechanism) the index has compared to MCWD and RAI.

Implications for estimating drought impacts on the carbon cycle of the Amazon rainforest

Drought leads to increased tree mortality and carbon losses in tropical forests (Hubau et al., 2020; Lewis et al., 2011; Phillips et al., 2009). With the prospect of more severe and frequent droughts in a future climate, more precise estimates of how much carbon is lost from reductions in growth and drought-induced mortality are necessary. Currently, the Amazon rainforest is acting as a carbon sink, thereby removing CO_2 from the atmosphere, but with more frequent and severe drought events, this sink is already declining (Hubau et al. 2020). Lewis et al. (2011) estimated a total loss of biomass for the Amazon basin in

2005 of 1.6 Pg C and a 38% more severe impact of 2.2 Pg C for 2010 based on TR6. When applied to the ΔMCWD derived from the precipitation datasets in our study, we calculate the loss of biomass of the 2005 drought event to be in the range of 1.3-1.8 Pg C, 1.5-2.3 Pg C in 2010 and 1.3-2.5 Pg C in 2016 (Fig. 4). This corresponds to approximately the average annual carbon uptake (1-2 PgC) per year, thus, turning the carbon sink into a carbon source. We acknowledge that our estimates are based on a relatively simple, empirically derived relation that does not take the biomass variability across the whole Amazon basin and individual forest/tree responses to drought into account. It however gives a rough estimate of potential carbon losses during drought and an idea of how much it varies depending on the precipitation datasets applied in a study. In addition, we would like to note that the empirical biomass MCWD relation from Lewis et al. (2011) has been estimated with constant ET=100 mm. When using evapotranspiration data (from ER5) for the calculation of MCWD, we find higher biomass losses (Fig. S2), and thus, the use of MCWD should be carefully viewed via its sensitivity to ET. In our analysis, MCWD appears to be robust against changes to some parameters, such as baseline period and inclusion/exclusion of drought years, but to be more sensitive to the evapotranspiration input.

Furthermore, our estimated carbon losses for the drought events might be underestimated as (1) the total duration of the drought was longer than 12 months (see above paragraph and Fig. 6) and can hence not be fully captured by the standard 12-month period of the MCWD calculation used in this study, and (2) potential lag effects through delayed plant mortality within the subsequent years are not considered so far. We would recommend for future studies to investigate the relationship of biomass losses with other drought indices (such as scPDSI) in a similar manner as done in Lewis et al. (2011). As the biomass of the Amazon rainforest is heterogeneously distributed (e.g. Saatchi et al., 2011), large-scale biomass loss induced by drought (i.e. severe ΔMCWD) should be interpreted carefully. Differences in the amount of biomass in different forest types, species composition and critical hydraulic processes should be considered when estimating potential biomass losses under drought stress. A step forward would be to use for example remotely sensed biomass maps to account for regional biomass distributions (e.g. Avitabile et al., 2016) or to simulate drought impacts with dynamic global vegetation models (DGVMs). DGVMs simulate the carbon- and water cycle of the biosphere in a process-based way, accounting for the interplay of carbon uptake and water loss through stomatal opening, evapotranspiration (ET), carbon assimilation via photosynthesis, and carbon allocation to different plant compartments such as leaves, wood, and roots (e.g. Schaphoff et al., 2018; Smith et al., 2014). The simulated response of tropical forests in DGVMs is particularly sensitive to precipitation input under present and future climate change scenarios (e.g. Seiler et al., 2015) and thus, it might be relevant to use multiple climate forcing datasets to test for climate data uncertainty. Particularly, studies based on ERI and TR6 should possibly be revisited and include another forcing dataset for their analysis.

Drought leads to increased tree mortality and carbon losses in tropical forests (Hubau et al., 2020; Lewis et al., 2011; Phillips et al., 2009). With the prospect of more severe and frequent droughts in a future climate, more precise estimates of how much carbon is lost from reductions in growth and drought-induced mortality are necessary. Currently, the Amazon rainforest is acting as a carbon sink, thereby removing CO_2 from the atmosphere, but with more frequent and severe drought events, this

4

sink is already declining (Hubau et al. 2020). Lewis et al. (2011) estimated a total loss of biomass for the Amazon basin in 2005 of 1.6 Pg C and a 38% more severe impact of 2.2 PgC for 2010 based on TRMM6. Later studies however found that the relationship between aMCWD and aAGB does not hold for the 2010 drought event (Feldpausch et al., 2016). When applied to the aMCWD derived from the precipitation datasets in our study, we still can calculate the loss of biomass of the 2005 drought event to be in the range of 0.7-1.7 PgC (Fig. 4). This is in the range of the regional average annual carbon uptake (1-2 PgC) per year, and thus, has the potential to turn the carbon sink into a carbon source. We acknowledge that our estimates are based on a relatively simple, empirically derived relation that does not take the biomass variability across the whole Amazon basin and individual forest/tree responses to drought into account. It however gives a rough estimation of potential carbon losses during drought and an idea of how much it varies depending on the precipitation datasets applied in a study. In addition, we would like to note that the empirical biomass aMCWD relation from Lewis et al. (2011) has been estimated with constant ET=100 mm. When using evapotranspiration data (from ERA5) for the calculation of aMCWD, we find generally lower biomass losses (between 10-20% lower, Fig. S3), and thus, the use of MCWD should be carefully viewed via its sensitivity to ET. While previous studies found that the MCWD calculation can be quite robust, in our analysis, MCWD is sensitive to the evapotranspiration input and baseline period (Fig. S3).

Furthermore, our totally affected areas (Fig. 2) for the drought events might be underestimated as (1) the total duration of the 2016 drought was longer than 12 months (see above paragraph and Fig. 6) and can hence not be fully captured by the standard 12-month period of the aMCWD and rMCWD calculation used in this study. (2) Potential lag effects due to delayed plant mortality within the subsequent years are not considered so far. We would recommend for future studies to investigate the relationship of biomass losses with other drought indices (such as scPDSI) in a similar manner as done in Lewis et al. (2011). As the biomass of the Amazon rainforest is heterogeneously distributed (e.g. Saatchi et al., 2011), large-scale drought-induced biomass losses which result from a severe aMCWD anomaly should be interpreted carefully. Differences in the amount of biomass in different forest types, species composition, and critical hydraulic processes should be considered when estimating potential biomass losses under drought stress (Feldpausch et al., 2016). A step forward would be to use, for example, remotely sensed biomass maps to account for regional biomass distributions (e.g. Avitabile et al., 2016) or to simulate drought impacts with dynamic global vegetation models (DGVMs). DGVMs simulate the carbon- and water cycle of the biosphere in a process-based way, accounting for the interplay of carbon uptake and water loss through stomatal opening, evapotranspiration (ET), carbon assimilation via photosynthesis, and carbon allocation to different plant compartments such as leaves, wood, and roots (e.g. Schaphoff et al., 2018; Smith et al., 2014). The simulated response of tropical forests in DGVMs is particularly sensitive to precipitation input under present and future climate change scenarios (e.g. Seiler et al., 2015). Therefore, we recommend using multiple climate forcing datasets to test for climate data uncertainty also under present climate conditions. Particularly, studies based on TRMM6 should possibly be revisited and complemented with more forcing datasets for their analysis.

6. Conclusions

We find substantial variation in the spatial extent, location, and timing of the extreme drought events in the years 2005, 2010 and 2016 in the Amazon basin. Depending on the precipitation dataset and drought index used the area affected by severe (extreme) drought varied between 0% and 39% (0% and 13.7%) for the 2016 event. Especially the area under severe drought conditions changed from almost no severe drought stress (5 out of 6 datasets) when using rRAI to greater than 10% when using rMCWD and $r$scPDS instead. The variation partly results from the application of different drought metrics (~~MCWD, RAI, scPDSI~~rMCWD, rRAI, $r$scPDSI) and from differences in the underlying precipitation datasets. Such differences also propagate when quantifying the impacts of ~~drought~~droughts on the carbon cycle of the Amazon rainforest and result in a large variability in biomass carbon losses~~, as we show in our analyses. This calls for the application of an ensemble of climate (~~ for a particular drought year. We found the biomass loss to vary between 0.7 and 1.6 PgC during the 2005 drought depending on the precipitation forcing.

We therefore recommend applying several climate (precipitation) datasets ~~and~~as well as drought metrics to account for model uncertainty when assessing the spatial extent, duration, and location of droughts. We regard it as an important step when assessing ~~the impacts of~~ drought impacts on tropical rainforests also under current climate conditions. Communicating the uncertainty in the estimation of drought events and their impacts on the Amazon rainforest is highly relevant and thus, multiple datasets should be applied by any large-scale study on drought impacts on vegetation.

7. Code availability

All scripts to reproduce analysis and figures are available at https://github.com/PhillipPapastefanou/DroughtAnalysis

8. Data availability

All datasets are available following the references in the method section.

9. Author contribution

P.P. and A.R. conceived the study and wrote the first draft of the manuscript. All authors contributed to the development of the analysis and the writing of the manuscript.

10. Competing interests

The authors declare no competing interests.

4

11. References

Albergel, C., Dutra, E., Munier, S., Calvet, J.-C., Munoz-Sabater, J., de Rosnay, P., & Balsamo, G. (2018). ERA-5 and ERA-Interim driven ISBA land surface model simulations: which one performs better? *Hydrology and Earth System Sciences*, *22*(6), 3515–3532. https://doi.org/10.5194/hess-22-3515-2018

Aragão, L. E. O. C., Malhi, Y., Roman-Cuesta, R. M., Saatchi, S., Anderson, L. O., & Shimabukuro, Y. E. (2007). Spatial patterns and fire response of recent Amazonian droughts. *Geophysical Research Letters*, *34*(7). https://doi.org/10.1029/2006GL028946

Avitabile, V., Herold, M., Heuvelink, G. B. M., Lewis, S. L., Phillips, O. L., Asner, G. P., Armston, J., Ashton, P. S., Banin, L., Bayol, N., Berry, N. J., Boeckx, P., de Jong, B. H. J., DeVries, B., Girardin, C. A. J., Kearsley, E., Lindsell, J. A., Lopez-Gonzalez, G., Lucas, R., … Willcock, S. (2016). An integrated pan-tropical biomass map using multiple reference datasets. *Global Change Biology*, *22*(4), 1406–1420. https://doi.org/10.1111/gcb.13139

Barkhordarian, A., Saatchi, S. S., Behrangi, A., Loikith, P. C., & Mechoso, C. R. (2019). A Recent Systematic Increase in Vapor Pressure Deficit over Tropical South America. *Scientific Reports*, *9*(1), 15331. https://doi.org/10.1038/s41598-019-51857-8

Blacutt, L. A., Herdies, D. L., de Gonçalves, L. G. G., Vila, D. A., & Andrade, M. (2015). Precipitation comparison for the CFSR, MERRA, TRMM3B42 and Combined Scheme datasets in Bolivia. *Atmospheric Research*, *163*, 117–131. https://doi.org/10.1016/j.atmosres.2015.02.002

Burton, C., Rifai, S., & Malhi, Y. (2018). Inter-comparison and assessment of gridded climate products over tropical forests during the 2015/2016 El Niño. *Philosophical Transactions of the Royal Society B: Biological Sciences*, *373*(1760), 20170406. https://doi.org/10.1098/rstb.2017.0406

Cai, W., Santoso, A., Wang, G., Yeh, S.-W. W., An, S.-I. Il, Cobb, K. M., Collins, M., Guilyardi, E., Jin, F.-F. F., Kug, J.-S. S., Lengaigne, M., McPhaden, M. J., Takahashi, K., Timmermann, A., Vecchi, G., Watanabe, M., & Wu, L. (2015). ENSO and greenhouse warming. *Nature Climate Change*, *5*(9), 849–859. https://doi.org/10.1038/nclimate2743

Castro, A. O., Chen, J., Zang, C. S., Shekhar, A., Jimenez, J. C., Bhattacharjee, S., Kindu, M., Morales, V. H., & Rammig, A. (2020). OCO-2 Solar-Induced Chlorophyll Fluorescence Variability across Ecoregions of the Amazon Basin and the Extreme Drought Effects of El Niño (2015–2016). *Remote Sensing*, *12*(7), 1202. https://doi.org/10.3390/rs12071202

Coelho, C. A. S., Cavalcanti, I. A. F., Costa, S. M. S., Freitas, S. R., Ito, E. R., Luz, G., Santos, A. F., Nobre, C. A., Marengo, J. A., & Pezza, A. B. (2012). Climate diagnostics of three major drought events in the Amazon and illustrations of their seasonal precipitation predictions. *Meteorological Applications*, *19*(2), 237–255. https://doi.org/10.1002/met.1324

Compo, G. P., Sardeshmukh, P. D., Whitaker, J. S., Brohan, P., Jones, P. D., & McColl, C. (2013). Independent confirmation of global land warming without the use of station temperatures. *Geophysical Research Letters*, *40*(12), 3170–3174. https://doi.org/10.1002/grl.50425

Covey, C., Gleckler, P. J., Doutriaux, C., Williams, D. N., Dai, A., Fasullo, J., Trenberth, K., & Berg, A. (2016). Metrics for the Diurnal Cycle of Precipitation: Toward Routine Benchmarks for Climate Models. *Journal of Climate*, *29*(12), 4461–4471. https://doi.org/10.1175/JCLI-D-15-0664.1

da Rocha, H. R., Goulden, M. L., Miller, S. D., Menton, M. C., Pinto, L. D. V. O., de Freitas, H. C., & e Silva Figueira, A. M. (2004). SEASONALITY OF WATER AND HEAT FLUXES OVER A TROPICAL FOREST IN EASTERN AMAZONIA. *Ecological Applications*, *14*(sp4), 22–32. https://doi.org/10.1890/02-6001

Dirmeyer, P. A., Cash, B. A., Kinter, J. L., Jung, T., Marx, L., Satoh, M., Stan, C., Tomita, H., Towers, P., Wedi, N., Achuthavarier, D., Adams, J. M., Altshuler, E. L., Huang, B., Jin, E. K., & Manganello, J. (2012). Simulating the diurnal cycle of rainfall in global climate models: resolution versus parameterization. *Climate Dynamics*, *39*(1–2), 399–418. https://doi.org/10.1007/s00382-011-1127-9

Dirmeyer, P. A., Schlosser, C. A., & Brubaker, K. L. (2009). Precipitation, Recycling, and Land Memory: An Integrated Analysis. *Journal of Hydrometeorology*, *10*(1), 278–288. https://doi.org/10.1175/2008JHM1016.1

Döll, P., & Lehner, B. (2002). Validation of a new global 30-min drainage direction map. *Journal of Hydrology*, *258*(1–4), 214–231. https://doi.org/10.1016/S0022-1694(01)00565-0

Espinoza, J. C., Sörensson, A. A., Ronchail, J., Molina-Carpio, J., Segura, H., Gutierrez-Cori, O., Ruscica, R., Condom, T., & Wongchuig-Correa, S. (2019). Regional hydro-climatic changes in the Southern Amazon Basin (Upper Madeira Basin) during the 1982–2017 period. *Journal of Hydrology: Regional Studies*, *26*(1), 100637. https://doi.org/10.1016/j.ejrh.2019.100637

Esquivel-Muelbert, A., Baker, T. R., Dexter, K. G., Lewis, S. L., Brienen, R. J. W., Feldpausch, T. R., Lloyd, J., Monteagudo-Mendoza, A., Arroyo, L., Álvarez-Dávila, E., Higuchi, N., Marimon, B. S., Marimon-Junior, B. H., Silveira, M., Vilanova, E., Gloor, E., Malhi, Y., Chave, J., Barlow, J., … Phillips, O. L. (2019). Compositional response of Amazon forests to climate change. *Global Change Biology*, *25*(1), 39–56. https://doi.org/10.1111/gcb.14413

Feldpausch, T. R., Phillips, O. L., Brienen, R. J. W., Gloor, E., Lloyd, J., Lopez-Gonzalez, G., Monteagudo-Mendoza, A., Malhi, Y., Alarcón, A., Álvarez Dávila, E., Alvarez-Loayza, P., Andrade, A., Aragao, L. E. O. C., Arroyo, L., Aymard C., G. A., Baker, T. R., Baraloto, C., Barroso, J., Bonal, D., … Vos, V. A. (2016). Amazon forest response to repeated droughts. *Global Biogeochemical Cycles*, *30*(7), 964–982. https://doi.org/10.1002/2015GB005133

Flack-Prain, S., Meir, P., Malhi, Y., Smallman, T. L., & Williams, M. (2019). The importance of physiological, structural and trait responses to drought stress in driving spatial and temporal variation in GPP across Amazon forests. *Biogeosciences*,

16(22), 4463–4484. https://doi.org/10.5194/bg-16-4463-2019

Forkel, M., Drüke, M., Thurner, M., Dorigo, W., Schaphoff, S., Thonicke, K., von Bloh, W., & Carvalhais, N. (2019). Constraining modelled global vegetation dynamics and carbon turnover using multiple satellite observations. *Scientific Reports*, *9*(1), 1–12. https://doi.org/10.1038/s41598-019-55187-7

Funk, C., Peterson, P., Landsfeld, M., Pedreros, D., Verdin, J., Shukla, S., Husak, G., Rowland, J., Harrison, L., Hoell, A., & Michaelsen, J. (2015). The climate hazards infrared precipitation with stations - A new environmental record for monitoring extremes. *Scientific Data*, *2*, 1–21. https://doi.org/10.1038/sdata.2015.66

Giardina, F., Konings, A. G., Kennedy, D., Alemohammad, S. H., Oliveira, R. S., Uriarte, M., & Gentine, P. (2018). Tall Amazonian forests are less sensitive to precipitation variability. *Nature Geoscience*, *11*(6), 405–409. https://doi.org/10.1038/s41561-018-0133-5

Giles, J. A., Ruscica, R. C., & Menéndez, C. G. (2020). The diurnal cycle of precipitation over South America represented by five gridded datasets. *International Journal of Climatology*, *40*(2), 668–686. https://doi.org/10.1002/joc.6229

Gloor, M., Barichivich, J., Ziv, G., Brienen, R., Schöngart, J., Peylin, P., Ladvocat Cintra, B. B., Feldpausch, T., Phillips, O., & Baker, J. (2015). Recent Amazon climate as background for possible ongoing and future changes of Amazon humid forests. *Global Biogeochemical Cycles*, *29*(9), 1384–1399. https://doi.org/10.1002/2014GB005080

Golian, S., Javadian, M., & Behrangi, A. (2019). On the use of satellite, gauge, and reanalysis precipitation products for drought studies. *Environmental Research Letters*, *14*(7). https://doi.org/10.1088/1748-9326/ab2203

Grossiord, C., Buckley, T. N., Cernusak, L. A., Novick, K. A., Poulter, B., Siegwolf, R. T. W., Sperry, J. S., & McDowell, N. G. (2020). Plant responses to rising vapor pressure deficit. *New Phytologist*, nph.16485. https://doi.org/10.1111/nph.16485

Harris, I., Jones, P. D. D., Osborn, T. J. J., & Lister, D. H. H. (2014). Updated high-resolution grids of monthly climatic observations - the CRU TS3.10 Dataset. *International Journal of Climatology*, *34*(3), 623–642. https://doi.org/10.1002/joc.3711

Hubau, W., Lewis, S. L., Phillips, O. L., Affum-Baffoe, K., Beeckman, H., Cuní-Sanchez, A., Daniels, A. K., Ewango, C. E. N., Fauset, S., Mukinzi, J. M., Sheil, D., Sonké, B., Sullivan, M. J. P., Sunderland, T. C. H., Taedoumg, H., Thomas, S. C., White, L. J. T., Abernethy, K. A., Adu-Bredu, S., … Zemagho, L. (2020). Asynchronous carbon sink saturation in African and Amazonian tropical forests. *Nature*, *579*(7797), 80–87. https://doi.org/10.1038/s41586-020-2035-0

Huffman, G. J., Bolvin, D. T., Nelkin, E. J., Wolff, D. B., Adler, R. F., Gu, G., Hong, Y., Bowman, K. P., & Stocker, E. F. (2007). The TRMM Multisatellite Precipitation Analysis (TMPA): Quasi-Global, Multiyear, Combined-Sensor

4

Precipitation Estimates at Fine Scales. *Journal of Hydrometeorology*, *8*(1), 38–55. https://doi.org/10.1175/JHM560.1

Jia, G., Shevliakova, E., Artaxo, P., de Noble-Ducoudre, N., Houghton, R., House, J., Kitajima, K., Lennard, C., Popp, A., Sirin, R., Sukumar, R., & Verchot, L. (2019). *Land–climate interactions. In: Climate Change and Land: an IPCC special report on climate change, desertification, land degradation, sustainable land management, food security, and greenhouse gas fluxes in terrestrial ecosystems*. https://www.ipcc.ch/site/assets/uploads/sites/4/2019/11/05_Chapter-2.pdf

Jiménez-Muñoz, J. C., Mattar, C., Barichivich, J., Santamaría-Artigas, A., Takahashi, K., Malhi, Y., Sobrino, J. A., & Schrier, G. Van Der. (2016). Record-breaking warming and extreme drought in the Amazon rainforest during the course of El Niño 2015–2016. *Scientific Reports*, *6*(1), 33130. https://doi.org/10.1038/srep33130

Jimenez, J. C., Barichivich, J., Mattar, C., Takahashi, K., Santamaría-Artigas, A., Sobrino, J. A., & Malhi, Y. (2018). Spatio-temporal patterns of thermal anomalies and drought over tropical forests driven by recent extreme climatic anomalies. *Philosophical Transactions of the Royal Society B: Biological Sciences*, *373*(1760), 20170300. https://doi.org/10.1098/rstb.2017.0300

Jimenez, J. C., Marengo, J. A., Alves, L. M., Sulca, J. C., Takahashi, K., Ferrett, S., & Collins, M. (2019). The role of ENSO flavours and TNA on recent droughts over Amazon forests and the Northeast Brazil region. *International Journal of Climatology*, *July*, 1–20. https://doi.org/10.1002/joc.6453

Koch, A., Hubau, W., & Lewis, S. L. (2021). Earth System Models Are Not Capturing Present-Day Tropical Forest Carbon Dynamics. *Earth's Future*, *9*(5), 1–19. https://doi.org/10.1029/2020EF001874

Konings, A. G., & Gentine, P. (2017). Global variations in ecosystem-scale isohydricity. *Global Change Biology*, *23*(2), 891–905. https://doi.org/10.1111/gcb.13389

Lewis, S. L., Brando, P. M., Phillips, O. L., Van Der Heijden, G. M. F., & Nepstad, D. (2011). The 2010 Amazon drought. *Science*, *331*(6017), 554. https://doi.org/10.1126/science.1200807

Malhi, Y., Aragao, L. E. O. C., Galbraith, D., Huntingford, C., Fisher, R., Zelazowski, P., Sitch, S., McSweeney, C., & Meir, P. (2009). Exploring the likelihood and mechanism of a climate-change-induced dieback of the Amazon rainforest. *Proceedings of the National Academy of Sciences*, *106*(49), 20610–20615. https://doi.org/10.1073/pnas.0804619106

Malhi, Yadvinder, Roberts, J. T., Betts, R. A., Killeen, T. J., Li, W., & Nobre, C. A. (2008). Climate Change, Deforestation, and the Fate of the Amazon. *Science*, *319*(5860), 169–172. https://doi.org/10.1126/science.1146961

Marengo, J. A., & Espinoza, J. C. (2016). Extreme seasonal droughts and floods in Amazonia: Causes, trends and impacts. *International Journal of Climatology*, *36*(3), 1033–1050. https://doi.org/10.1002/joc.4420

4

Marengo, J. A., Nobre, C. A., Tomasella, J., Cardoso, M. F., & Oyama, M. D. (2008). Hydro-climatic and ecological behaviour of the drought of Amazonia in 2005. *Philosophical Transactions of the Royal Society B: Biological Sciences*, *363*(1498), 1773–1778. https://doi.org/10.1098/rstb.2007.0015

Marengo, José A., Nobre, C. A., Tomasella, J., Oyama, M. D., Sampaio de Oliveira, G., de Oliveira, R., Camargo, H., Alves, L. M., & Brown, I. F. (2008). The Drought of Amazonia in 2005. *Journal of Climate*, *21*(3), 495–516. https://doi.org/10.1175/2007JCLI1600.1

Marengo, Jose A., Tomasella, J., Alves, L. M., Soares, W. R., & Rodriguez, D. A. (2011). The drought of 2010 in the context of historical droughts in the Amazon region. *Geophysical Research Letters*, *38*(12), n/a-n/a. https://doi.org/10.1029/2011GL047436

Miralles, D. G., Gentine, P., Seneviratne, S. I., & Teuling, A. J. (2019). Land–atmospheric feedbacks during droughts and heatwaves: state of the science and current challenges. *Annals of the New York Academy of Sciences*, *1436*(1), 19–35. https://doi.org/10.1111/nyas.13912

Muñoz-Sabater, J., Dutra, E., Balsamo, G., Boussetta, S., Zsoter, E., Albergel, C., & Agusti-Panareda, A. (2018). *ERA5-Land: an improved version of the ERA5 reanalysis land component*.

Phillips, O. L., Aragao, L. E. O. C., Lewis, S. L., Fisher, J. B., Lloyd, J., Lopez-Gonzalez, G., Malhi, Y., Monteagudo, A., Peacock, J., Quesada, C. A., van der Heijden, G., Almeida, S., Amaral, I., Arroyo, L., Aymard, G., Baker, T. R., Banki, O., Blanc, L., Bonal, D., … Torres-Lezama, A. (2009). Drought Sensitivity of the Amazon Rainforest. *Science*, *323*(5919), 1344–1347. https://doi.org/10.1126/science.1164033

Rao, K., Anderegg, W. R. L., Sala, A., Martínez-Vilalta, J., & Konings, A. G. (2019). Satellite-based vegetation optical depth as an indicator of drought-driven tree mortality. *Remote Sensing of Environment*, *227*(February), 125–136. https://doi.org/10.1016/j.rse.2019.03.026

Rifai, S. W., Li, S., & Malhi, Y. (2019). Coupling of El Niño events and long-term warming leads to pervasive climate extremes in the terrestrial tropics. *Environmental Research Letters*, *14*(10), 105002. https://doi.org/10.1088/1748-9326/ab402f

Rodell, M., Houser, P. R., Jambor, U., Gottschalck, J., Mitchell, K., Meng, C.-J., Arsenault, K., Cosgrove, B., Radakovich, J., Bosilovich, M., Entin, J. K., Walker, J. P., Lohmann, D., & Toll, D. (2004). The Global Land Data Assimilation System. *Bulletin of the American Meteorological Society*, *85*(3), 381–394. https://doi.org/10.1175/BAMS-85-3-381

Ruida, Z., Chen, X., Wang, Z., Lai, C., & Goddard, S. (2018). *Package scPDSI* (0.1.3). https://github.com/Sibada/scPDSI

Ruiz-Vásquez, M., Arias, P. A., Martínez, J. A., & Espinoza, J. C. (2020). Effects of Amazon basin deforestation on regional atmospheric circulation and water vapor transport towards tropical South America. *Climate Dynamics*, *0123456789*.

4

https://doi.org/10.1007/s00382-020-05223-4

Schaphoff, S., Von Bloh, W., Rammig, A., Thonicke, K., Biemans, H., Forkel, M., Gerten, D., Heinke, J., Jägermeyr, J., Knauer, J., Langerwisch, F., Lucht, W., Müller, C., Rolinski, S., & Waha, K. (2018). LPJmL4 - A dynamic global vegetation model with managed land - Part 1: Model description. *Geoscientific Model Development*, *11*(4), 1343–1375. https://doi.org/10.5194/gmd-11-1343-2018

Schneider, U., Becker, A., Finger, P., Anja, M.-C., & Markus, Z. (2018). *GPCC Full Data Monthly Version 2018.0 at 0.5°: Monthly Land-Surface Precipitation from Rain-Gauges built on GTS-based and Historic Data*. Global Precipitation Climatology Centre (GPCC, http://gpcc.dwd.de/) at Deutscher Wetterdienst. https://doi.org/10.5676/DWD_GPCC/FD_M_V2018_050

Seiler, C., Hutjes, R. W. A., Kruijt, B., & Hickler, T. (2015). The sensitivity of wet and dry tropical forests to climate change in Bolivia. *Journal of Geophysical Research: Biogeosciences*, *120*(3), 399–413. https://doi.org/10.1002/2014JG002749

Seto, S., Iguchi, T., & Meneghini, R. (2011). Comparison of TRMM PR V6 and V7 focusing heavy rainfall. *2011 IEEE International Geoscience and Remote Sensing Symposium*, *22760365*, 2582–2585. https://doi.org/10.1109/IGARSS.2011.6049769

Sheffield, J., Goteti, G., & Wood, E. F. (2006). Development of a 50-Year High-Resolution Global Dataset of Meteorological Forcings for Land Surface Modeling. *Journal of Climate*, *19*(13), 3088–3111. https://doi.org/10.1175/JCLI3790.1

Smith, B., Wårlind, D., Arneth, A., Hickler, T., Leadley, P., Siltberg, J., & Zaehle, S. (2014). Implications of incorporating N cycling and N limitations on primary production in an individual-based dynamic vegetation model. *Biogeosciences*, *11*(7), 2027–2054. https://doi.org/10.5194/bg-11-2027-2014

Sörensson, A. A., & Ruscica, R. C. (2018). Intercomparison and Uncertainty Assessment of Nine Evapotranspiration Estimates Over South America. *Water Resources Research*, *54*(4), 2891–2908. https://doi.org/10.1002/2017WR021682

Stephenson, N. (1998). Actual evapotranspiration and deficit: biologically meaningful correlates of vegetation distribution across spatial scales. *Journal of Biogeography*, *25*(5), 855–870. https://doi.org/10.1046/j.1365-2699.1998.00233.x

van der Ent, R. J., Savenije, H. H. G., Schaefli, B., & Steele-Dunne, S. C. (2010). Origin and fate of atmospheric moisture over continents. *Water Resources Research*, *46*(9), 1–12. https://doi.org/10.1029/2010WR009127

Viovy, N. (2018). *CRUNCEP Version 7 - Atmospheric Forcing Data for the Community Land Model*. Research Data Archive at the National Center for Atmospheric Research, Computational and Information Systems Laboratory. http://rda.ucar.edu/datasets/ds314.3/%22

Fo

Fo
Unt
Rah
Zer

von Randow, C., Manzi, A. O., Kruijt, B., de Oliveira, P. J., Zanchi, F. B., Silva, R. L., Hodnett, M. G., Gash, J. H. C., Elbers, J. A., Waterloo, M. J., Cardoso, F. L., & Kabat, P. (2004). Comparative measurements and seasonal variations in energy and carbon exchange over forest and pasture in South West Amazonia. *Theoretical and Applied Climatology*, *78*(1–3), 5–26. https://doi.org/10.1007/s00704-004-0041-z

Weedon, G. P., Gomes, S., Viterbo, P., Shuttleworth, W. J., Blyth, E., Österle, H., Adam, J. C., Bellouin, N., Boucher, O., & Best, M. (2011). Creation of the WATCH Forcing Data and Its Use to Assess Global and Regional Reference Crop Evaporation over Land during the Twentieth Century. *Journal of Hydrometeorology*, *12*(5), 823–848. https://doi.org/10.1175/2011JHM1369.1

Weedon, Graham P, Balsamo, G., Bellouin, N., Gomes, S., Best, M. J., & Viterbo, P. (2014). Data methodology applied to ERA-Interim reanalysis data. *Water Resources Research*, *50*, 7505–7514. https://doi.org/10.1002/2014WR015638.Received

Wells, N., Goddard, S., & Hayes, M. J. (2004). A Self-Calibrating Palmer Drought Severity Index. *Journal of Climate*, *17*(12), 2335–2351. https://doi.org/10.1175/1520-0442(2004)017<2335:ASPDSI>2.0.CO;2

Willmott, C. J., Rowe, C. M., & Philpot, W. D. (1985). Small-Scale Climate Maps: A Sensitivity Analysis of Some Common Assumptions Associated with Grid-Point Interpolation and Contouring. *The American Cartographer*, *12*(1), 5–16. https://doi.org/10.1559/152304085783914686

Yang, H., Piao, S., Zeng, Z., Ciais, P., Yin, Y., Friedlingstein, P., Sitch, S., Ahlström, A., Guimberteau, M., Huntingford, C., Levis, S., Levy, P. E., Huang, M., Li, Y., Li, X., Lomas, M. R., Peylin, P., Poulter, B., Viovy, N., … Wang, L. (2015). Multicriteria evaluation of discharge simulation in Dynamic Global Vegetation Models. *Journal of Geophysical Research: Atmospheres*, *120*(15), 7488–7505. https://doi.org/10.1002/2015JD023129

Yang, J., Tian, H., Pan, S., Chen, G., Zhang, B., & Dangal, S. (2018). Amazon drought and forest response: Largely reduced forest photosynthesis but slightly increased canopy greenness during the extreme drought of 2015/2016. *Global Change Biology*, *24*(5), 1919–1934. https://doi.org/10.1111/gcb.14056

Zang, C. S., Buras, A., Esquivel-Muelbert, A., Jump, A. S., Rigling, A., & Rammig, A. (2020). Standardized drought indices in ecological research: Why one size does not fit all. *Global Change Biology*, *26*(2), 322–324. https://doi.org/10.1111/gcb.14809

Zemp, D. C., Schleussner, C.-F., Barbosa, H. M. J., & Rammig, A. (2017). Deforestation effects on Amazon forest resilience. *Geophysical Research Letters*, *44*(12), 6182–6190. https://doi.org/10.1002/2017GL072955

Zemp, D. C., Schleussner, C.-F., Barbosa, H. M. J., van der Ent, R. J., Donges, J. F., Heinke, J., Sampaio, G., & Rammig, A. (2014). On the importance of cascading moisture recycling in South America. *Atmospheric Chemistry and Physics*, *14*(23), 13337–13359. https://doi.org/10.5194/acp-14-13337-2014

4

Zemp, Delphine Clara, Schleussner, C.-F., Barbosa, H. M. J., Hirota, M., Montade, V., Sampaio, G., Staal, A., Wang-Erlandsson, L., & Rammig, A. (2017). Self-amplified Amazon forest loss due to vegetation-atmosphere feedbacks. *Nature Communications*, *8*(1), 14681. https://doi.org/10.1038/ncomms14681

Zeng, N., Yoon, J.-H., Marengo, J. A., Subramaniam, A., Nobre, C. A., Mariotti, A., & Neelin, J. D. (2008). Causes and impacts of the 2005 Amazon drought. *Environmental Research Letters*, *3*(1), 014002. https://doi.org/10.1088/1748-9326/3/1/014002

Ziese, M., Schneider, U., Meyer-Christoffer, A., Schamm, K., Vido, J., Finger, P., Bissolli, P., Pietzsch, S., & Becker, A. (2014). The GPCC Drought Index – a new, combined and gridded global drought index. *Earth System Science Data*, *6*(2), 285–295. https://doi.org/10.5194/essd-6-285-2014

1930

1935

Tables

Precipitation dataset	Abbreviation	Details	Resolutions	Derived from	References
Climate Hazards group Infrared Precipitation with Stations	CHIRPS	quasi-global (50°S-50°N)	high resolution (0.05°), daily, pentadal, and monthly	Remote sensing, in-situ observations	Funk et al., 2015
Tropical Rainfall Measurement Misson	TRMM v6 3b43	quasi-global (50°S-50°N)	Quarter degree resolution (0.25°) daily, pentadal, and monthly	Remote sensing	Huffman et al., 2007
Tropical Rainfall Measurement Misson	TRMM v7 3B43	quasi-global (50°S-50°N)	Quarter degree resolution (0.25°), daily, pentadal, and monthly	Remote sensing	Huffman et al., 2007
	CRU_NCEP V8	global	Half degree resolution (0.5°), daily, pentadal and monthly	Mainly in-situ observations	Viovy et al., 2017
ERA5		global	Quarter degree resolution (0.25°), sub-daily, daily, monthly	Land surface models, remote sensing, in-situ observations	Albergel et al., 2018
Global Land Data Assimilation System	GLDAS 2.1	global	Quarter degree resolution (0.25°), daily, pentadal, and monthly	Land surface models	Rodell et al., 2004

Global Precipitation Climatology Centre at Deutscher Wetterdienst	GPCC2018	global	Quarter degree resolution (0.25°), monthly	in-situ observations	Schneider et al., 2018
Global Soil Wetness Project Phase 3	GSWP3	global	Half degree resolution (0.5°), daily, monthly	Land surface models, remote sensing, in-situ observations	H. Kim et al. n.d.; http://hydro.iis.u-tokyo.ac.jp/GSWP3/index.html
WATCH Forcing Data (WFD) + WATCH Forcing Data methodology applied to ERA-Interim data (WFDEI)	WATCH WFDEI	global	Half degree resolution (0.5°), daily, monthly	Land surface models, remote sensing, in-situ observations	Weedon et al., 2011, 2014

Table 1: Overview of the 10 precipitation datasets used in our study.

Adler, R. F., Huffman, G. J., Chang, A., Ferraro, R., Xie, P.-P., Janowiak, J., Rudolf, B., Schneider, U., Curtis, S., Bolvin, D., Gruber, A., Susskind, J., Arkin, P. and Nelkin, E.: The Version 2 Global Precipitation Climatology Project (GPCP) Monthly Precipitation Analysis (1979 Present), J. Hydrometeorol., 4(6), 1147 1167, doi:10.1175/1525 7541(2003)004<1147:TVGPCP>2.0.CO;2, 2003.

Albergel, C., Dutra, E., Munier, S., Calvet, J. C., Munoz Sabater, J., de Rosnay, P. and Balsamo, G.: ERA 5 and ERA Interim driven ISBA land surface model simulations: which one performs better?, Hydrol. Earth Syst. Sci., 22(6), 3515 3532, doi:10.5194/hess 22 3515 2018, 2018.

Aragão, L. E. O. C., Malhi, Y., Roman Cuesta, R. M., Saatchi, S., Anderson, L. O. and Shimabukuro, Y. E.: Spatial patterns and fire response of recent Amazonian droughts, Geophys. Res. Lett., 34(7), doi:10.1029/2006GL028946, 2007.

1950

1955

Avitabile, V., Herold, M., Heuvelink, G. B. M., Lewis, S. L., Phillips, O. L., Asner, G. P., Armston, J., Ashton, P. S., Banin, L., Bayol, N., Berry, N. J., Boeckx, P., de Jong, B. H. J., DeVries, B., Girardin, C. A. J., Kearsley, E., Lindsell, J. A., Lopez-Gonzalez, G., Lucas, R., Malhi, Y., Morel, A., Mitchard, E. T. A., Nagy, L., Qie, L., Quinones, M. J., Ryan, C. M., Ferry, S. J. W., Sunderland, T., Laurin, G. V., Gatti, R. C., Valentini, R., Verbeeck, H., Wijaya, A. and Willcock, S.: An integrated pan-tropical biomass map using multiple reference datasets, Glob. Chang. Biol., 22(4), 1406–1420, doi:10.1111/gcb.13139, 2016.

Barkhordarian, A., Saatchi, S. S., Behrangi, A., Loikith, P. C. and Mechoso, C. R.: A Recent Systematic Increase in Vapor Pressure Deficit over Tropical South America, Sci. Rep., 9(1), 15331, doi:10.1038/s41598-019-51857-8, 2019.

Blacutt, L. A., Herdies, D. L., de Gonçalves, L. G. G., Vila, D. A. and Andrade, M.: Precipitation comparison for the CFSR, MERRA, TRMM3B42 and Combined Scheme datasets in Bolivia, Atmos. Res., 163, 117–131, doi:10.1016/j.atmosres.2015.02.002, 2015.

Burton, C., Rifai, S. and Malhi, Y.: Inter-comparison and assessment of gridded climate products over tropical forests during the 2015/2016 El Niño, Philos. Trans. R. Soc. B Biol. Sci., 373(1760), 20170406, doi:10.1098/rstb.2017.0406, 2018.

Cai, W., Santoso, A., Wang, G., Yeh, S. W. W., An, S. I. Il, Cobb, K. M., Collins, M., Guilyardi, E., Jin, F. F. F., Kug, J. S. S., Lengaigne, M., McPhaden, M. J., Takahashi, K., Timmermann, A., Vecchi, G., Watanabe, M. and Wu, L.: ENSO and greenhouse warming, Nat. Clim. Chang., 5(9), 849–859, doi:10.1038/nclimate2743, 2015.

Castro, A. O., Chen, J., Zang, C. S., Shekhar, A., Jimenez, J. C., Bhattacharjee, S., Kindu, M., Morales, V. H. and Rammig, A.: OCO-2 Solar-Induced Chlorophyll Fluorescence Variability across Ecoregions of the Amazon Basin and the Extreme Drought Effects of El Niño (2015–2016), Remote Sens., 12(7), 1202, doi:10.3390/rs12071202, 2020.

Coelho, C. A. S., Cavalcanti, I. A. F., Costa, S. M. S., Freitas, S. R., Ito, E. R., Luz, G., Santos, A. F., Nobre, C. A., Marengo, J. A. and Pezza, A. B.: Climate diagnostics of three major drought events in the Amazon and illustrations of their seasonal precipitation predictions, Meteorol. Appl., 19(2), 237–255, doi:10.1002/met.1324, 2012.

Compo, G. P., Sardeshmukh, P. D., Whitaker, J. S., Brohan, P., Jones, P. D. and McColl, C.: Independent confirmation of global land warming without the use of station temperatures, Geophys. Res. Lett., 40(12), 3170–3174, doi:10.1002/grl.50425, 2013.

Covey, C., Gleckler, P. J., Doutriaux, C., Williams, D. N., Dai, A., Fasullo, J., Trenberth, K. and Berg, A.: Metrics for the Diurnal Cycle of Precipitation: Toward Routine Benchmarks for Climate Models, J. Clim., 29(12), 4461–4471, doi:10.1175/JCLI-D-15-0664.1, 2016.

Dee, D. P., Uppala, S. M., Simmons, A. J., Berrisford, P., Poli, P., Kobayashi, S., Andrae, U., Balmaseda, M. A., Balsamo, G., Bauer, P., Bechtold, P., Beljaars, A. C. M., van de Berg, L., Bidlot, J., Bormann, N., Delsol, C., Dragani, R., Fuentes, M., Geer, A. J., Haimberger, L., Healy, S. B., Hersbach, H., Hólm, E. V., Isaksen, L., Kållberg, P., Köhler, M., Matricardi, M., McNally, A. P., Monge-Sanz, B. M., Morcrette, J. J., Park, B. K., Peubey, C., de Rosnay, P., Tavolato, C., Thépaut, J. N. and

4

Vitart, F.: The ERA-Interim reanalysis: configuration and performance of the data assimilation system, Q. J. R. Meteorol. Soc., 137(656), 553–597, doi:10.1002/qj.828, 2011.

Dirmeyer, P. A., Schlosser, C. A. and Brubaker, K. L.: Precipitation, Recycling, and Land Memory: An Integrated Analysis, J. Hydrometeorol., 10(1), 278–288, doi:10.1175/2008JHM1016.1, 2009.

Dirmeyer, P. A., Cash, B. A., Kinter, J. L., Jung, T., Marx, L., Satoh, M., Stan, C., Tomita, H., Towers, P., Wedi, N., Achuthavarier, D., Adams, J. M., Altshuler, E. L., Huang, B., Jin, E. K. and Manganello, J.: Simulating the diurnal cycle of rainfall in global climate models: resolution versus parameterization, Clim. Dyn., 39(1–2), 399–418, doi:10.1007/s00382-011-1127-9, 2012.

Döll, P. and Lehner, B.: Validation of a new global 30-min drainage direction map, J. Hydrol., 258(1–4), 214–231, doi:10.1016/S0022-1694(01)00565-0, 2002.

van der Ent, R. J., Savenije, H. H. G., Schaefli, B. and Steele Dunne, S. C.: Origin and fate of atmospheric moisture over continents, Water Resour. Res., 46(9), 1–12, doi:10.1029/2010WR009127, 2010.

Espinoza, J. C., Sörensson, A. A., Ronchail, J., Molina Carpio, J., Segura, H., Gutierrez Cori, O., Ruscica, R., Condom, T. and Wongchuig Correa, S.: Regional hydro-climatic changes in the Southern Amazon Basin (Upper Madeira Basin) during the 1982–2017 period, J. Hydrol. Reg. Stud., 26(1), 100637, doi:10.1016/j.ejrh.2019.100637, 2019.

Esquivel-Muelbert, A., Baker, T. R., Dexter, K. G., Lewis, S. L., Brienen, R. J. W., Feldpausch, T. R., Lloyd, J., Monteagudo-Mendoza, A., Arroyo, L., Álvarez Dávila, E., Higuchi, N., Marimon, B. S., Marimon Junior, B. H., Silveira, M., Vilanova, E., Gloor, E., Malhi, Y., Chave, J., Barlow, J., Bonal, D., Davila Cardozo, N., Erwin, T., Fauset, S., Hérault, B., Laurance, S., Poorter, L., Qie, L., Stahl, C., Sullivan, M. J. P., ter Steege, H., Vos, V. A., Zuidema, P. A., Almeida, E., Almeida de Oliveira, E., Andrade, A., Vieira, S. A., Aragão, L., Araujo-Murakami, A., Arets, E., Aymard C, G. A., Baraloto, C., Camargo, P. B., Barroso, J. G., Bongers, F., Boot, R., Camargo, J. L., Castro, W., Chama Moscoso, V., Comiskey, J., Cornejo Valverde, F., Lola da Costa, A. C., del Aguila Pasquel, J., Di Fiore, A., Fernanda Duque, L., Elias, F., Engel, J., Flores Llampazo, G., Galbraith, D., Herrera Fernández, R., Honorio Coronado, E., Hubau, W., Jimenez Rojas, E., Lima, A. J. N., Umetsu, R. K., Laurance, W., Lopez Gonzalez, G., Lovejoy, T., Aurelio Melo Cruz, O., Morandi, P. S., Neill, D., Núñez Vargas, P., Pallqui Camacho, N. C., Parada Gutierrez, A., Pardo, G., Peacock, J., Peña Claros, M., Peñuela Mora, M. C., Petronelli, P., Pickavance, G. C., Pitman, N., Prieto, A., Quesada, C., Ramírez Angulo, H., Réjou Méchain, M., Restrepo Correa, Z., Roopsind, A., Rudas, A., Salomão, R., Silva, N., Silva Espejo, J., Singh, J., Stropp, J., Terborgh, J., Thomas, R., Toledo, M., Torres Lezama, A., Valenzuela Gamarra, L., van de Meer, P. J., van der Heijden, G., et al.: Compositional response of Amazon forests to climate change, Glob. Chang. Biol., 25(1), 39–56, doi:10.1111/gcb.14413, 2019.

Forkel, M., Drüke, M., Thurner, M., Dorigo, W., Schaphoff, S., Thonicke, K., von Bloh, W. and Carvalhais, N.: Constraining modelled global vegetation dynamics and carbon turnover using multiple satellite observations, Sci. Rep., 9(1), 1–12, doi:10.1038/s41598-019-55187-7, 2019.

Funk, C., Peterson, P., Landsfeld, M., Pedreros, D., Verdin, J., Shukla, S., Husak, G., Rowland, J., Harrison, L., Hoell, A. and

Michaelsen, J.: The climate hazards infrared precipitation with stations - A new environmental record for monitoring extremes, Sci. Data, 2, 1–21, doi:10.1038/sdata.2015.66, 2015.

Giardina, F., Konings, A. G., Kennedy, D., Alemohammad, S. H., Oliveira, R. S., Uriarte, M. and Gentine, P.: Tall Amazonian forests are less sensitive to precipitation variability, Nat. Geosci., 11(6), 405–409, doi:10.1038/s41561-018-0133-5, 2018.

Giles, J. A., Ruscica, R. C. and Menéndez, C. G.: The diurnal cycle of precipitation over South America represented by five gridded datasets, Int. J. Climatol., 40(2), 668–686, doi:10.1002/joc.6229, 2020.

Di Giuseppe, F., Molteni, F. and Dutra, E.: Real-time correction of ERA-Interim monthly rainfall, Geophys. Res. Lett., 40(14), 3750–3755, doi:10.1002/grl.50670, 2013.

Gloor, M., Barichivich, J., Ziv, G., Brienen, R., Schöngart, J., Peylin, P., Ladvocat Cintra, B. B., Feldpausch, T., Phillips, O. and Baker, J.: Recent Amazon climate as background for possible ongoing and future changes of Amazon humid forests, Global Biogeochem. Cycles, 29(9), 1384–1399, doi:10.1002/2014GB005080, 2015.

Golian, S., Javadian, M. and Behrangi, A.: On the use of satellite, gauge, and reanalysis precipitation products for drought studies, Environ. Res. Lett., 14(7), doi:10.1088/1748-9326/ab2203, 2019.

Grossiord, C., Buckley, T. N., Cernusak, L. A., Novick, K. A., Poulter, B., Siegwolf, R. T. W., Sperry, J. S. and McDowell, N. G.: Plant responses to rising vapor pressure deficit, New Phytol., nph.16485, doi:10.1111/nph.16485, 2020.

Harris, I., Jones, P. D. D., Osborn, T. J. J. and Lister, D. H. H.: Updated high-resolution grids of monthly climatic observations - the CRU TS3.10 Dataset, Int. J. Climatol., 34(3), 623–642, doi:10.1002/joc.3711, 2014.

Hubau, W., Lewis, S. L., Phillips, O. L., Affum-Baffoe, K., Beeckman, H., Cuní-Sanchez, A., Daniels, A. K., Ewango, C. E. N., Fauset, S., Mukinzi, J. M., Sheil, D., Sonké, B., Sullivan, M. J. P., Sunderland, T. C. H., Taedoumg, H., Thomas, S. C., White, L. J. T., Abernethy, K. A., Adu-Bredu, S., Amani, C. A., Baker, T. R., Banin, L. F., Baya, F., Begne, S. K., Bennett, A. C., Benedet, F., Bitariho, R., Bocko, Y. E., Boeckx, P., Boundja, P., Brienen, R. J. W., Brncic, T., Chezeaux, E., Chuyong, G. B., Clark, C. J., Collins, M., Comiskey, J. A., Coomes, D. A., Dargie, G. C., de Haulleville, T., Kamdem, M. N. D., Doucet, J. L., Esquivel-Muelbert, A., Feldpausch, T. R., Fofanah, A., Foli, E. G., Gilpin, M., Gloor, E., Gonmadje, C., Gourlet-Fleury, S., Hall, J. S., Hamilton, A. C., Harris, D. J., Hart, T. B., Hockemba, M. B. N., Hladik, A., Ifo, S. A., Jeffery, K. J., Jucker, T., Yakusu, E. K., Kearsley, E., Kenfack, D., Koch, A., Leal, M. E., Levesley, A., Lindsell, J. A., Lisingo, J., Lopez-Gonzalez, G., Lovett, J. C., Makana, J. R., Malhi, Y., Marshall, A. R., Martin, J., Martin, E. H., Mbayu, F. M., Medjibe, V. P., Mihindou, V., Mitchard, E. T. A., Moore, S., Munishi, P. K. T., Bengone, N. N., Ojo, L., Ondo, F. E., Peh, K. S. H., Pickavance, G. C., Poulsen, A. D., Poulsen, J. R., Qie, L., Reitsma, J., Rovero, F., Swaine, M. D., Talbot, J., Taplin, J., Taylor, D. M., Thomas, D. W., Toirambe, B., Mukendi, J. T., Tuagben, D., Umunay, P. M., et al.: Asynchronous carbon sink saturation in African and Amazonian tropical forests, Nature, 579(7797), 80–87, doi:10.1038/s41586-020-2035-0, 2020.

Huffman, G. J., Bolvin, D. T., Nelkin, E. J., Wolff, D. B., Adler, R. F., Gu, G., Hong, Y., Bowman, K. P. and Stocker, E. F.:

The TRMM Multisatellite Precipitation Analysis (TMPA): Quasi-Global, Multiyear, Combined-Sensor Precipitation Estimates at Fine Scales, J. Hydrometeorol., 8(1), 38–55, doi:10.1175/JHM560.1, 2007.

2180 Jia, G., Shevliakova, E., Artaxo, P., de Noble-Ducoudre, N., Houghton, R., House, J., Kitajima, K., Lennard, C., Popp, A., Sirin, R., Sukumar, R. and Verchot, L.: Land–climate interactions. In: Climate Change and Land: an IPCC special report on climate change, desertification, land degradation, sustainable land management, food security, and greenhouse gas fluxes in terrestrial ecosystems, [online] Available from: https://www.ipcc.ch/site/assets/uploads/sites/4/2019/11/05_Chapter-2.pdf, 2019.

2185 Jiménez-Muñoz, J. C., Mattar, C., Barichivich, J., Santamaría-Artigas, A., Takahashi, K., Malhi, Y., Sobrino, J. A. and Schrier, G. Van Der: Record-breaking warming and extreme drought in the Amazon rainforest during the course of El Niño 2015–2016, Sci. Rep., 6(1), 33130, doi:10.1038/srep33130, 2016.

Jimenez, J. C., Barichivich, J., Mattar, C., Takahashi, K., Santamaría-Artigas, A., Sobrino, J. A. and Malhi, Y.: Spatio-temporal patterns of thermal anomalies and drought over tropical forests driven by recent extreme climatic anomalies, Philos. Trans. R. 2190 Soc. B Biol. Sci., 373(1760), 20170300, doi:10.1098/rstb.2017.0300, 2018.

Jimenez, J. C., Marengo, J. A., Alves, L. M., Sulca, J. C., Takahashi, K., Ferrett, S. and Collins, M.: The role of ENSO flavours and TNA on recent droughts over Amazon forests and the Northeast Brazil region, Int. J. Climatol., (July), 1–20, doi:10.1002/joc.6453, 2019.

Konings, A. G. and Gentine, P.: Global variations in ecosystem-scale isohydricity, Glob. Chang. Biol., 23(2), 891–905, 2195 doi:10.1111/gcb.13389, 2017.

Lewis, S. L., Brando, P. M., Phillips, O. L., Van Der Heijden, G. M. F. and Nepstad, D.: The 2010 Amazon drought, Science (80-.)., 331(6017), 554, doi:10.1126/science.1200807, 2011.

Maignan, F., Bréon, F. M., Chevallier, F., Viovy, N., Ciais, P., Garrec, C., Trules, J. and Mancip, M.: Evaluation of a Global Vegetation Model using time series of satellite vegetation indices, Geosci. Model Dev., 4(4), 1103–1114, doi:10.5194/gmd-4-2200 1103-2011, 2011.

Malhi, Y., Roberts, J. T., Betts, R. A., Killeen, T. J., Li, W. and Nobre, C. A.: Climate Change, Deforestation, and the Fate of the Amazon, Science (80-.)., 319(5860), 169–172, doi:10.1126/science.1146961, 2008.

Malhi, Y., Aragao, L. E. O. C., Galbraith, D., Huntingford, C., Fisher, R., Zelazowski, P., Sitch, S., McSweeney, C. and Meir, P.: Exploring the likelihood and mechanism of a climate-change-induced dieback of the Amazon rainforest, Proc. Natl. Acad. 2205 Sci., 106(49), 20610–20615, doi:10.1073/pnas.0804619106, 2009.

Marengo, J. A. and Espinoza, J. C.: Extreme seasonal droughts and floods in Amazonia: Causes, trends and impacts, Int. J.

4

Climatol., 36(3), 1033–1050, doi:10.1002/joc.4420, 2016.

Marengo, J. A., Nobre, C. A., Tomasella, J., Cardoso, M. F. and Oyama, M. D.: Hydro-climatic and ecological behaviour of the drought of Amazonia in 2005, Philos. Trans. R. Soc. B Biol. Sci., 363(1498), 1773–1778, doi:10.1098/rstb.2007.0015, 2008a.

Marengo, J. A., Nobre, C. A., Tomasella, J., Oyama, M. D., Sampaio de Oliveira, G., de Oliveira, R., Camargo, H., Alves, L. M. and Brown, I. F.: The Drought of Amazonia in 2005, J. Clim., 21(3), 495–516, doi:10.1175/2007JCLI1600.1, 2008b.

Marengo, J. A., Tomasella, J., Alves, L. M., Soares, W. R. and Rodriguez, D. A.: The drought of 2010 in the context of historical droughts in the Amazon region, Geophys. Res. Lett., 38(12), n/a-n/a, doi:10.1029/2011GL047436, 2011.

Miralles, D. G., Gentine, P., Seneviratne, S. I. and Teuling, A. J.: Land-atmospheric feedbacks during droughts and heatwaves: state of the science and current challenges, Ann. N. Y. Acad. Sci., 1436(1), 19–35, doi:10.1111/nyas.13912, 2019.

Muñoz-Sabater, J., Dutra, E., Balsamo, G., Boussetta, S., Zsoter, E., Albergel, C. and Agusti-Panareda, A.: ERA5-Land: an improved version of the ERA5 reanalysis land component, 2018.

Phillips, O. L., Aragao, L. E. O. C., Lewis, S. L., Fisher, J. B., Lloyd, J., Lopez-Gonzalez, G., Malhi, Y., Monteagudo, A., Peacock, J., Quesada, C. A., van der Heijden, G., Almeida, S., Amaral, I., Arroyo, L., Aymard, G., Baker, T. R., Banki, O., Blanc, L., Bonal, D., Brando, P., Chave, J., de Oliveira, A. C. A., Cardozo, N. D., Czimczik, C. I., Feldpausch, T. R., Freitas, M. A., Gloor, E., Higuchi, N., Jimenez, E., Lloyd, G., Meir, P., Mendoza, C., Morel, A., Neill, D. A., Nepstad, D., Patino, S., Penuela, M. C., Prieto, A., Ramirez, F., Schwarz, M., Silva, J., Silveira, M., Thomas, A. S., Steege, H. t., Stropp, J., Vasquez, R., Zelazowski, P., Davila, E. A., Andelman, S., Andrade, A., Chao, K. J., Erwin, T., Di Fiore, A., C., E. H., Keeling, H., Killeen, T. J., Laurance, W. F., Cruz, A. P., Pitman, N. C. A., Vargas, P. N., Ramirez-Angulo, H., Rudas, A., Salamao, R., Silva, N., Terborgh, J. and Torres-Lezama, A.: Drought Sensitivity of the Amazon Rainforest, Science (80-.)., 323(5919), 1344–1347, doi:10.1126/science.1164033, 2009.

Poulter, B., Frank, D. C., Hodson, E. L. and Zimmermann, N. E.: Impacts of land cover and climate data selection on understanding terrestrial carbon dynamics and the CO 2 airborne fraction, Biogeosciences, 8(8), 2027–2036, doi:10.5194/bg-8-2027-2011, 2011.

von Randow, C., Manzi, A. O., Kruijt, B., de Oliveira, P. J., Zanchi, F. B., Silva, R. L., Hodnett, M. G., Gash, J. H. C., Elbers, J. A., Waterloo, M. J., Cardoso, F. L. and Kabat, P.: Comparative measurements and seasonal variations in energy and carbon exchange over forest and pasture in South West Amazonia, Theor. Appl. Climatol., 78(1–3), 5–26, doi:10.1007/s00704-004-0041-z, 2004.

Rao, K., Anderegg, W. R. L., Sala, A., Martínez-Vilalta, J. and Konings, A. G.: Satellite-based vegetation optical depth as an indicator of drought-driven tree mortality, Remote Sens. Environ., 227(February), 125–136, doi:10.1016/j.rse.2019.03.026, 2019.

Rifai, S. W., Li, S. and Malhi, Y.: Coupling of El Niño events and long-term warming leads to pervasive climate extremes in the terrestrial tropics, Environ. Res. Lett., 14(10), 105002, doi:10.1088/1748-9326/ab402f, 2019.

da Rocha, H. R., Goulden, M. L., Miller, S. D., Menton, M. C., Pinto, L. D. V. O., de Freitas, H. C. and e Silva Figueira, A. M.: SEASONALITY OF WATER AND HEAT FLUXES OVER A TROPICAL FOREST IN EASTERN AMAZONIA, Ecol. Appl., 14(sp4), 22–32, doi:10.1890/02-6001, 2004.

Rodell, M., Houser, P. R., Jambor, U., Gottschalck, J., Mitchell, K., Meng, C. J., Arsenault, K., Cosgrove, B., Radakovich, J., Bosilovich, M., Entin, J. K., Walker, J. P., Lohmann, D. and Toll, D.: The Global Land Data Assimilation System, Bull. Am. Meteorol. Soc., 85(3), 381–394, doi:10.1175/BAMS-85-3-381, 2004.

Ruida, Z., Chen, X., Wang, Z., Lai, C. and Goddard, S.: Package scPDSI, [online] Available from: https://github.com/Sibada/scPDSI, 2018.

Ruiz Vásquez, M., Arias, P. A., Martínez, J. A. and Espinoza, J. C.: Effects of Amazon basin deforestation on regional atmospheric circulation and water vapor transport towards tropical South America, Clim. Dyn., (0123456789), doi:10.1007/s00382-020-05223-4, 2020.

Schaphoff, S., Von Bloh, W., Rammig, A., Thonicke, K., Biemans, H., Forkel, M., Gerten, D., Heinke, J., Jägermeyr, J., Knauer, J., Langerwisch, F., Lucht, W., Müller, C., Rolinski, S. and Waha, K.: LPJmL4 - A dynamic global vegetation model with managed land - Part 1: Model description, Geosci. Model Dev., 11(4), 1343–1375, doi:10.5194/gmd-11-1343-2018, 2018.

Schneider, U., Becker, A., Finger, P., Anja, M. C. and Markus, Z.: GPCC Full Data Monthly Version 2018.0 at 0.5°: Monthly Land Surface Precipitation from Rain Gauges built on GTS-based and Historic Data, , doi:10.5676/DWD_GPCC/FD_M_V2018_050, 2018.

Seiler, C., Hutjes, R. W. A., Kruijt, B. and Hickler, T.: The sensitivity of wet and dry tropical forests to climate change in Bolivia, J. Geophys. Res. Biogeosciences, 120(3), 399–413, doi:10.1002/2014JG002749, 2015.

Seto, S., Iguchi, T. and Meneghini, R.: Comparison of TRMM PR V6 and V7 focusing heavy rainfall, in 2011 IEEE International Geoscience and Remote Sensing Symposium, pp. 2582–2585, IEEE., 2011.

Sheffield, J., Goteti, G. and Wood, E. F.: Development of a 50-Year High-Resolution Global Dataset of Meteorological Forcings for Land Surface Modeling, J. Clim., 19(13), 3088–3111, doi:10.1175/JCLI3790.1, 2006.

Smith, B., Wårlind, D., Arneth, A., Hickler, T., Leadley, P., Siltberg, J. and Zaehle, S.: Implications of incorporating N cycling and N limitations on primary production in an individual-based dynamic vegetation model, Biogeosciences, 11(7), 2027–2054, doi:10.5194/bg-11-2027-2014, 2014.

4

Sörensson, A. A. and Ruscica, R. C.: Intercomparison and Uncertainty Assessment of Nine Evapotranspiration Estimates Over South America, Water Resour. Res., 54(4), 2891–2908, doi:10.1002/2017WR021682, 2018.

Toomey, M., D. A. Roberts, C. Still, M. L. Goulden, and J. P. McFadden (2011), Remotely sensed heat anomalies linked with Amazonian forest biomass declines, Geophys. Res. Lett., 38, L19704, doi:10.1029/2011GL049041.

Viovy, N.: CRUNCEP Version 7 - Atmospheric Forcing Data for the Community Land Model, [online] Available from: http://rda.ucar.edu/datasets/ds314.3/%22, 2018.

Weedon, G. P., Gomes, S., Viterbo, P., Shuttleworth, W. J., Blyth, E., Österle, H., Adam, J. C., Bellouin, N., Boucher, O. and Best, M.: Creation of the WATCH Forcing Data and Its Use to Assess Global and Regional Reference Crop Evaporation over Land during the Twentieth Century, J. Hydrometeorol., 12(5), 823–848, doi:10.1175/2011JHM1369.1, 2011.

Weedon, G. P., Balsamo, G., Bellouin, N., Gomes, S., Best, M. J. and Viterbo, P.: Data methodology applied to ERA-Interim reanalysis data, Water Resour. Res., 50, 7505–7514, doi:10.1002/2014WR015638.Received, 2014.

Wells, N., Goddard, S. and Hayes, M. J.: A Self-Calibrating Palmer Drought Severity Index, J. Clim., 17(12), 2335–2351, doi:10.1175/1520-0442(2004)017<2335:ASPDSI>2.0.CO;2, 2004.

Willmott, C. J., Rowe, C. M. and Philpot, W. D.: Small-Scale Climate Maps: A Sensitivity Analysis of Some Common Assumptions Associated with Grid Point Interpolation and Contouring, Am. Cartogr., 12(1), 5–16, doi:10.1559/152304085783914686, 1985.

Yang, H., Piao, S., Zeng, Z., Ciais, P., Yin, Y., Friedlingstein, P., Sitch, S., Ahlström, A., Guimberteau, M., Huntingford, C., Levis, S., Levy, P. E., Huang, M., Li, Y., Li, X., Lomas, M. R., Peylin, P., Poulter, B., Viovy, N., Zaehle, S., Zeng, N., Zhao, F. and Wang, L.: Multicriteria evaluation of discharge simulation in Dynamic Global Vegetation Models, J. Geophys. Res. Atmos., 120(15), 7488–7505, doi:10.1002/2015JD023129, 2015.

Yang, J., Tian, H., Pan, S., Chen, G., Zhang, B. and Dangal, S.: Amazon drought and forest response: Largely reduced forest photosynthesis but slightly increased canopy greenness during the extreme drought of 2015/2016, Glob. Chang. Biol., 24(5), 1919–1934, doi:10.1111/gcb.14056, 2018.

Zang, C. S., Buras, A., Esquivel-Muelbert, A., Jump, A. S., Rigling, A. and Rammig, A.: Standardized drought indices in ecological research: Why one size does not fit all, Glob. Chang. Biol., 26(2), 322–324, doi:10.1111/gcb.14809, 2020.

Zemp, D. C., Schleussner, C. F., Barbosa, H. M. J., van der Ent, R. J., Donges, J. F., Heinke, J., Sampaio, G. and Rammig, A.: On the importance of cascading moisture recycling in South America, Atmos. Chem. Phys., 14(23), 13337–13359, doi:10.5194/acp-14-13337-2014, 2014.

4

2395   Zemp, D. C., Schleussner, C.-F., Barbosa, H. M. J. and Rammig, A.: Deforestation effects on Amazon forest resilience, Geophys. Res. Lett., 44(12), 6182–6190, doi:10.1002/2017GL072955, 2017a.

Zemp, D. C., Schleussner, C. F., Barbosa, H. M. J., Hirota, M., Montade, V., Sampaio, G., Staal, A., Wang-Erlandsson, L. and Rammig, A.: Self-amplified Amazon forest loss due to vegetation-atmosphere feedbacks, Nat. Commun., 8(1), 14681, doi:10.1038/ncomms14681, 2017b.

2400   Zeng, N., Yoon, J. H., Marengo, J. A., Subramaniam, A., Nobre, C. A., Mariotti, A. and Neelin, J. D.: Causes and impacts of the 2005 Amazon drought, Environ. Res. Lett., 3(1), 014002, doi:10.1088/1748-9326/3/1/014002, 2008.

Ziese, M., Schneider, U., Meyer-Christoffer, A., Schamm, K., Vido, J., Finger, P., Bissolli, P., Pietzsch, S. and Becker, A.: The GPCC Drought Index — a new, combined and gridded global drought index, Earth Syst. Sci. Data, 6(2), 285–295, doi:10.5194/essd-6-285-2014, 2014.

2405

Columns show the name of the dataset, the official abbreviation, the spatial and temporal resolution, the inputs the precipitation datasets are derived from, and the references.

Fo

For
Unt
Rah
Zer
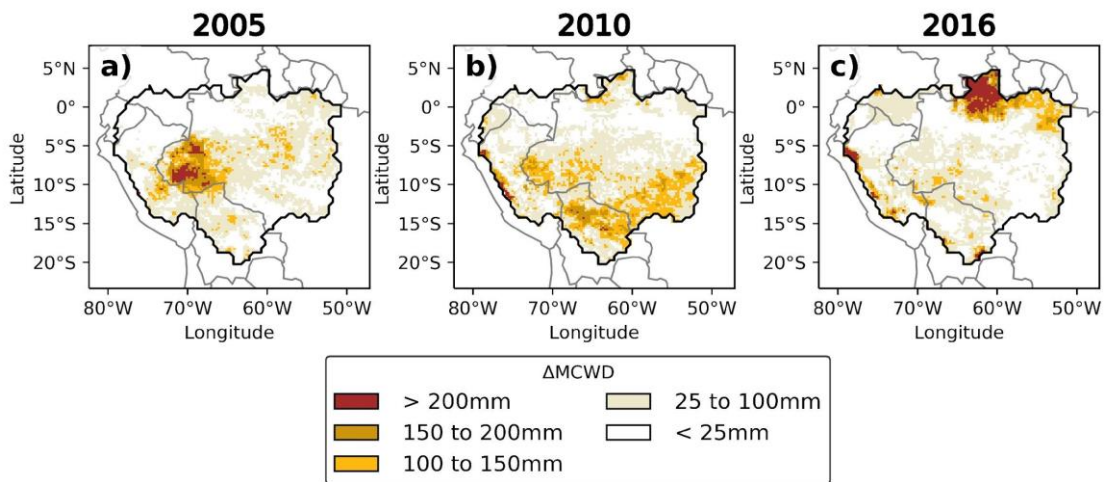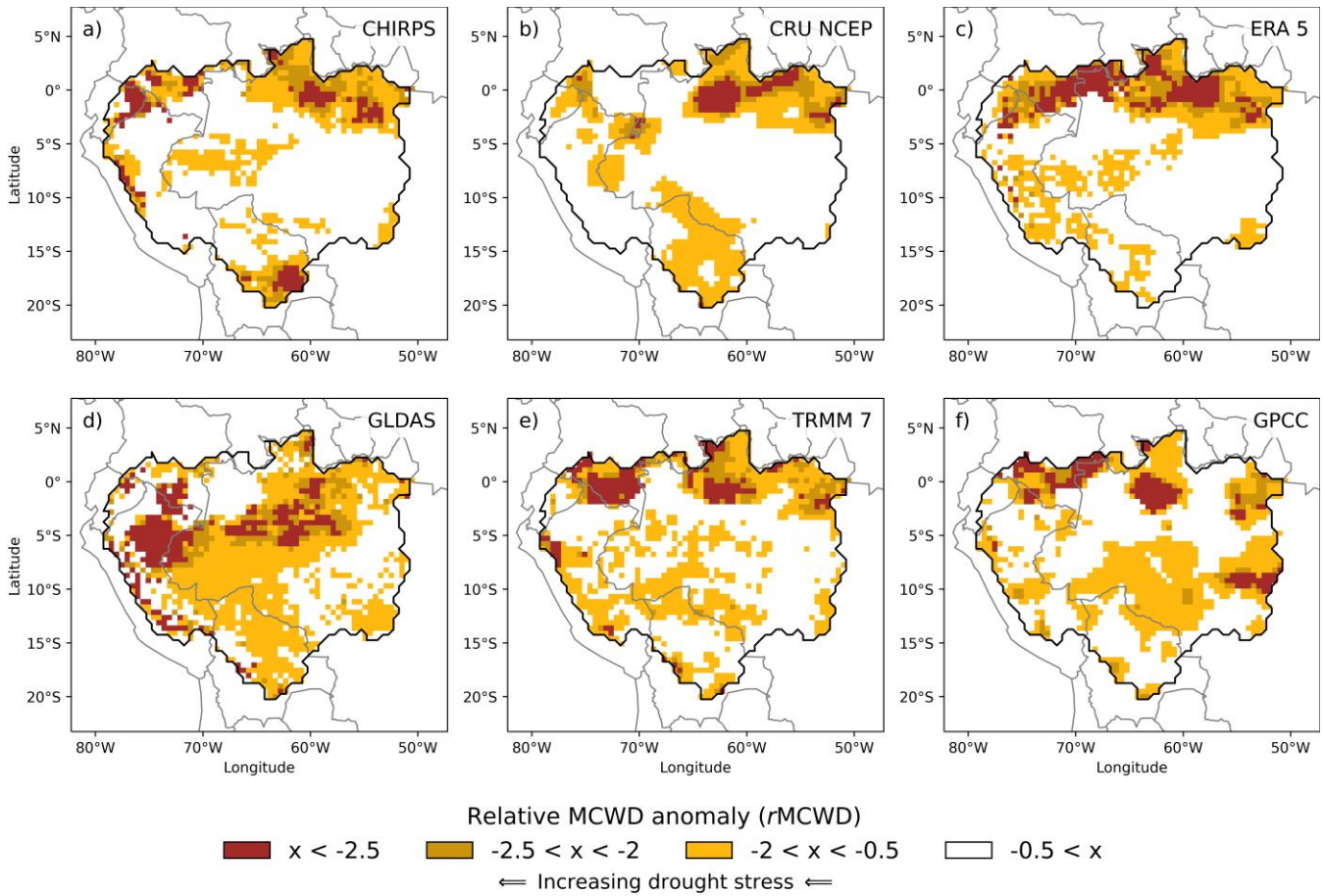
Figures

Figure 1: ~~(a-e) Anomalies of ΔMCWD~~**Relative MCWD anomalies** (from October to September) as an indicator for drought stress in the Amazon ~~Basin~~**basin** during the record-breaking drought ~~events in 2005, 2010 and 2015/16 based on the TR7 dataset~~**event in 2016. Displayed are only the datasets that include the year 2016 in their temporal range. The baseline period of the MCWD calculation is 2001 to 2016.**
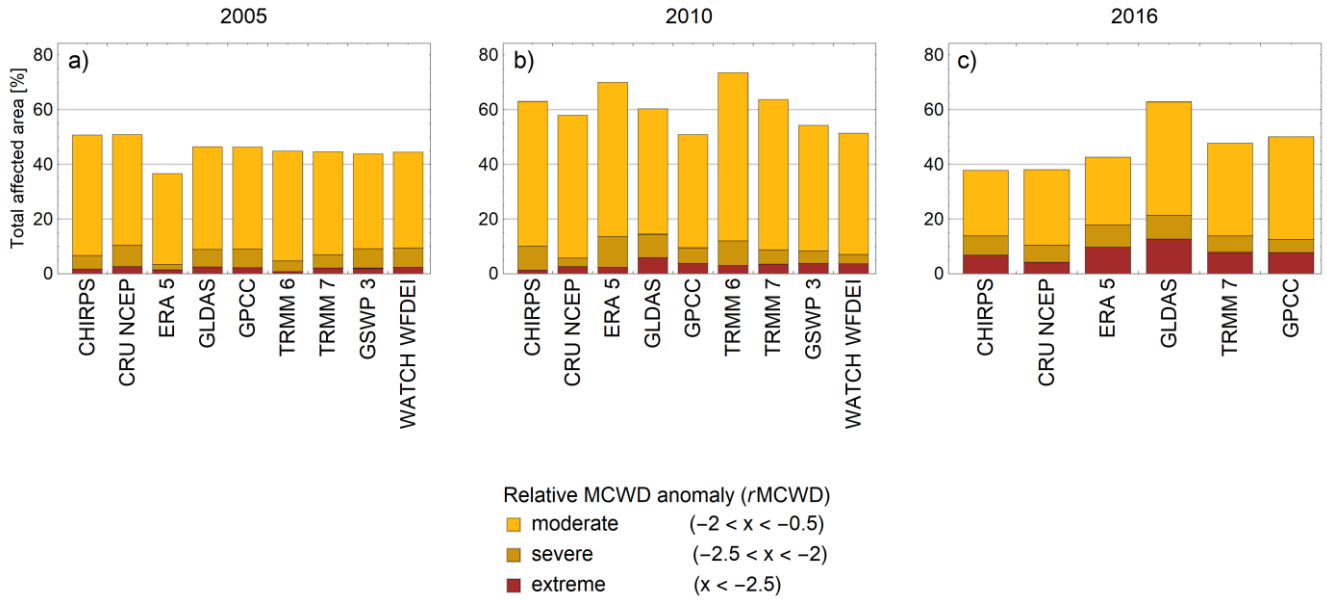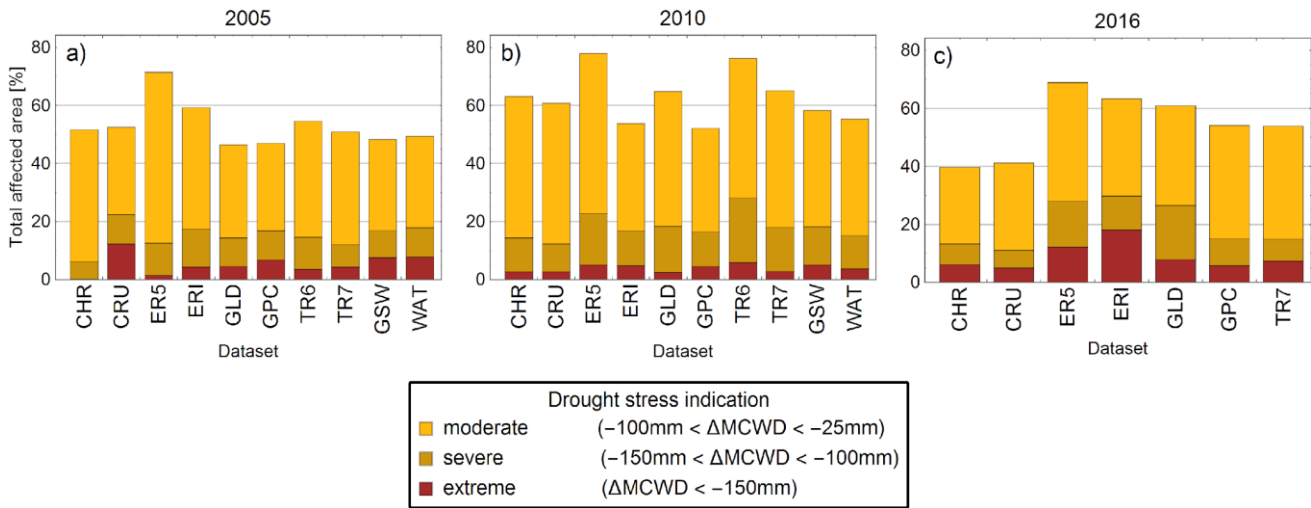
Figure 2: Total area of the Amazon basin affected by drought stress (%) according to ~~ΔMCWD~~**relative MCWD anomaly** for each of the precipitation datasets ~~(for abbreviations see Tab. 1)~~. **Displayed are the three drought events (a) 2005, (b) 2010 and (c) 2016. The total area representing the Amazon basin in our study is 5.94 million km². For absolute area affected, see Tab. ~~2~~S2 and ~~3~~S3.**
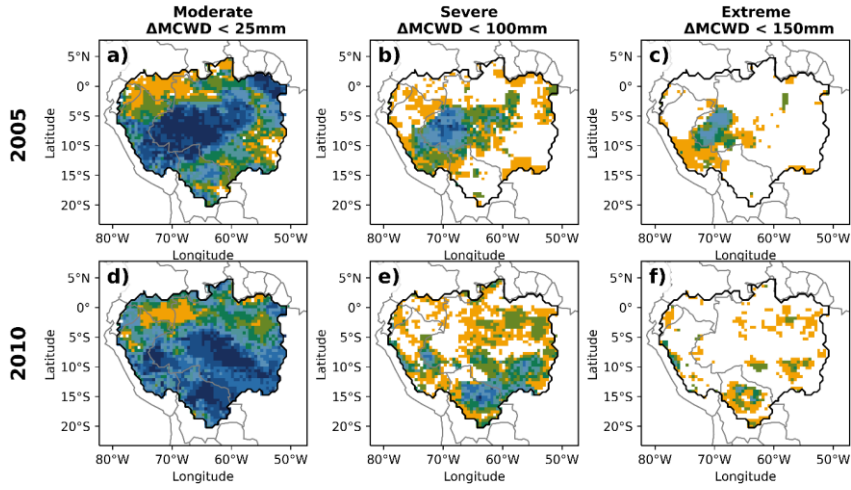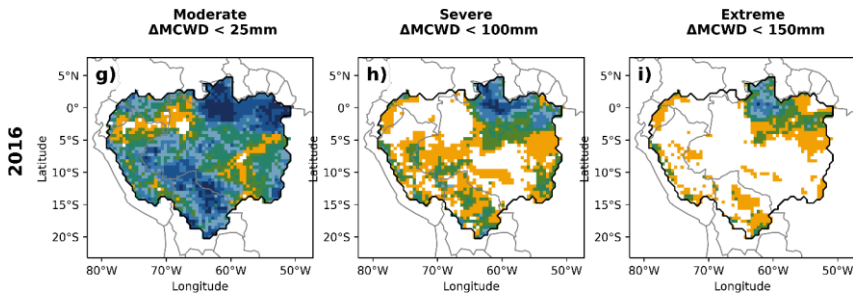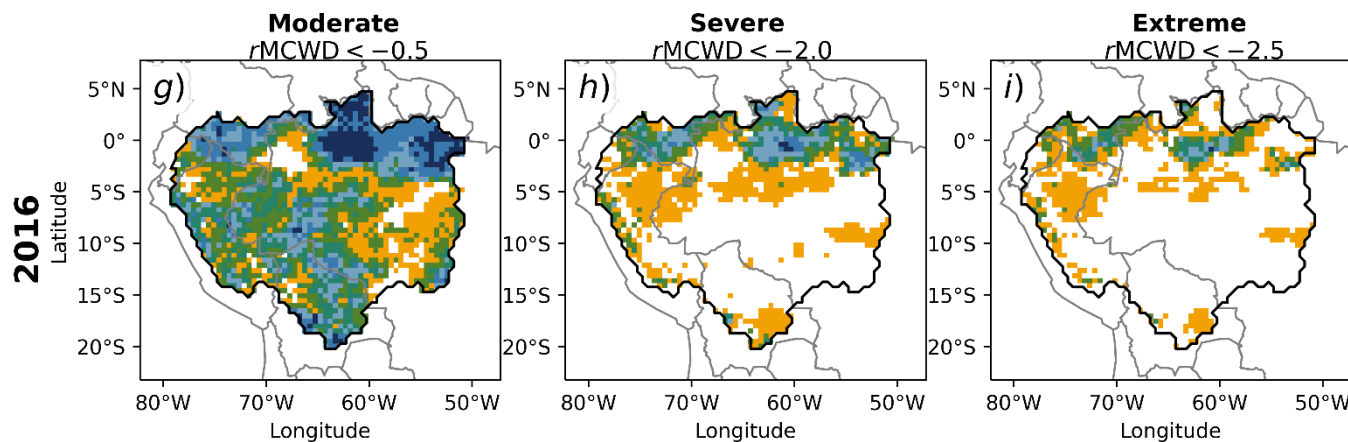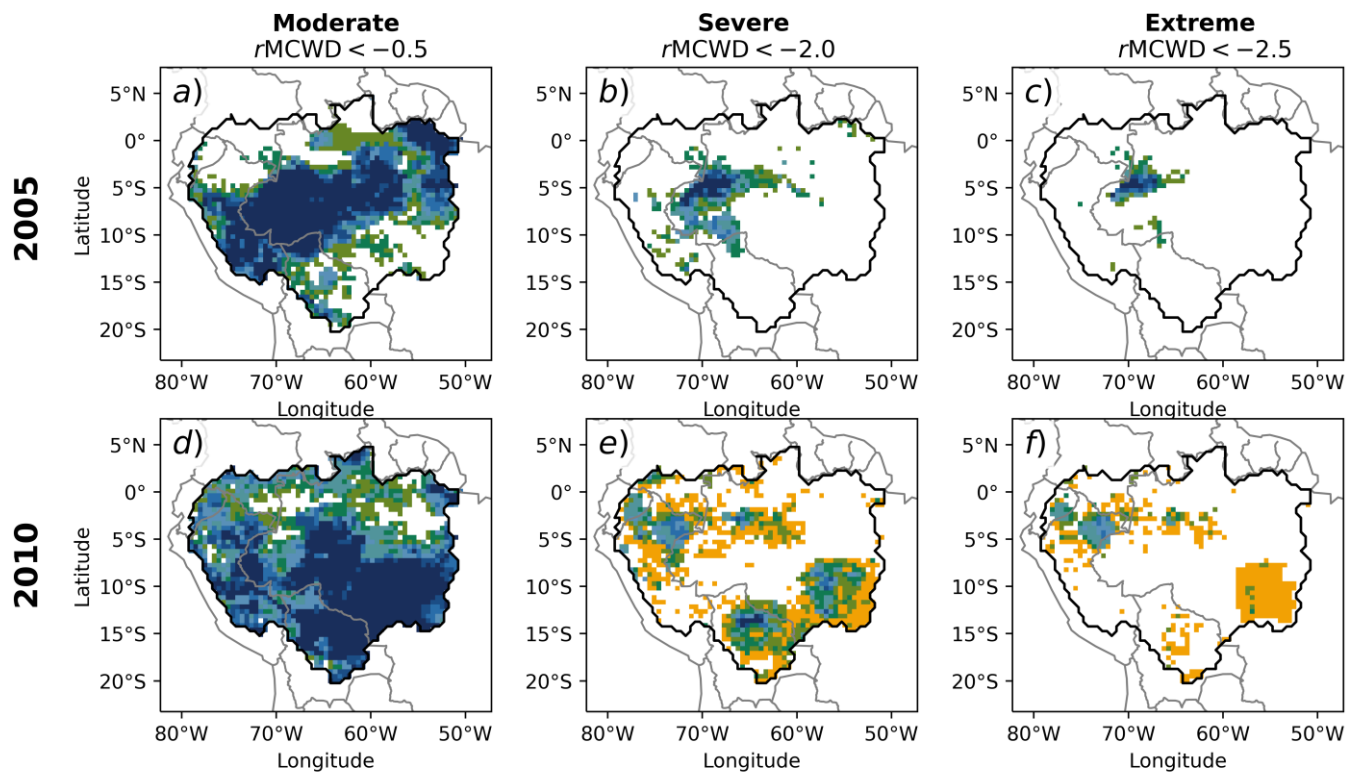
Figure 3: **Agreement of precipitation datasets on drought area as identified by** ~~AMCWD~~**relative MCWD** **anomalies. In columns, different levels of drought severity are displayed and rows show the different drought years 2005 (a-c), 2010**

(d-f) and 2016 (g-i). The colors indicate the number of datasets that agree on a specific drought level in a given pixel. Drought severity levels are defined as moderate (~~AMCWD < 25mm),~~*r*MCWD < -0.5), severe (~~AMCWD < 100mm~~*r*MCWD < -2.0) and extreme (~~AMCWD < 150mm~~*r*MCWD < -2.5). Orange pixels indicate areas where only one dataset shows the respective drought stress (No agreement = "None"). White pixels represent areas where no dataset shows any drought signal. Note that in a-f, ~~TR6~~TRMM 6 and ~~GSW~~GSWP3 were excluded, as they were either very similar to its successor (~~TR7) and~~TRMM 7) or due to a similar reanalysis procedure (~~WAT~~WATCH_WFDEI). In g-i, only ~~seven~~six datasets were included, which cover the full time period until 2016.
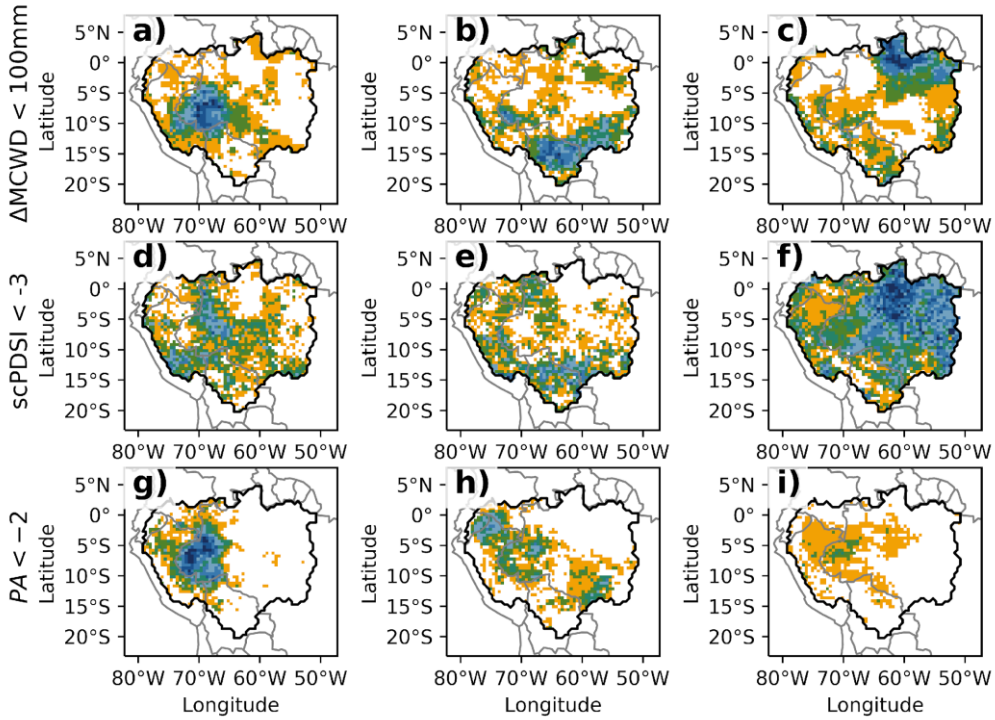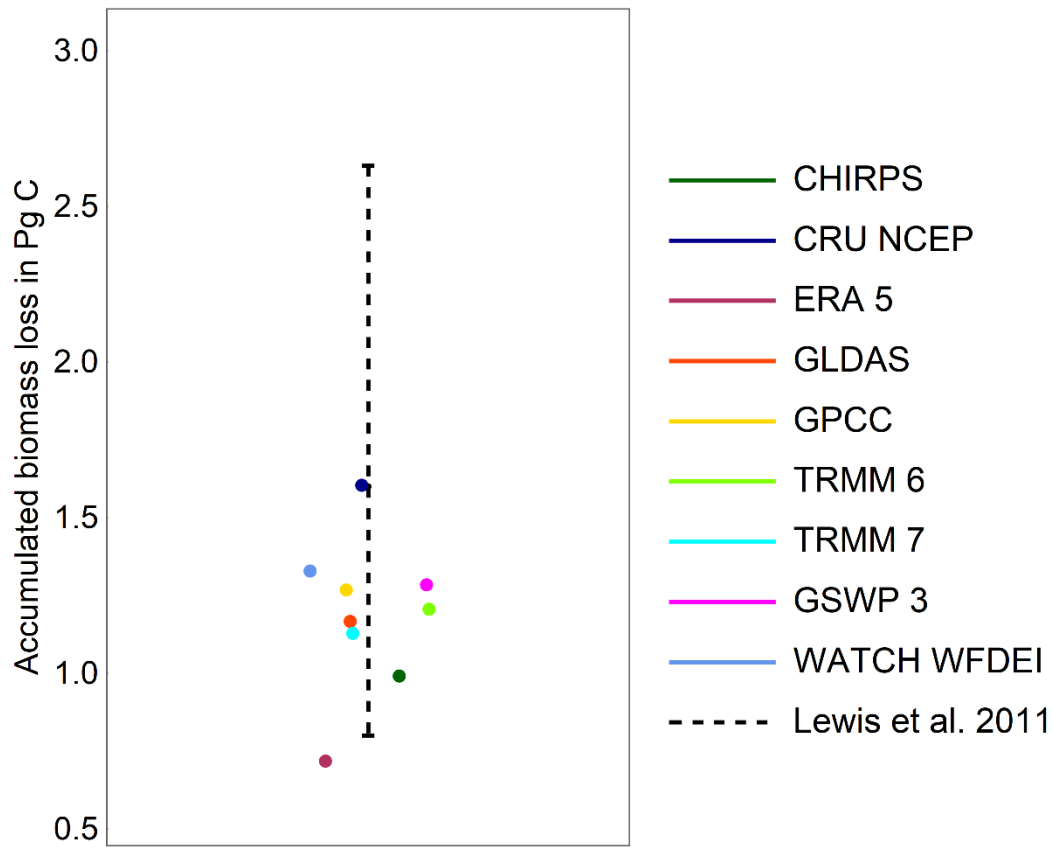
Figure 4

Figure 4: Impact of the 2005 drought event on aboveground carbon biomass (aAGB anomaly in PgC). Biomass loss was calculated for each of the precipitation datasets (colored dots) based on a linear relation between biomass loss and *a*MCWD as proposed by Lewis et al. (2011). The dashed lines indicate the range of estimated carbon losses from Lewis et al. (2011).
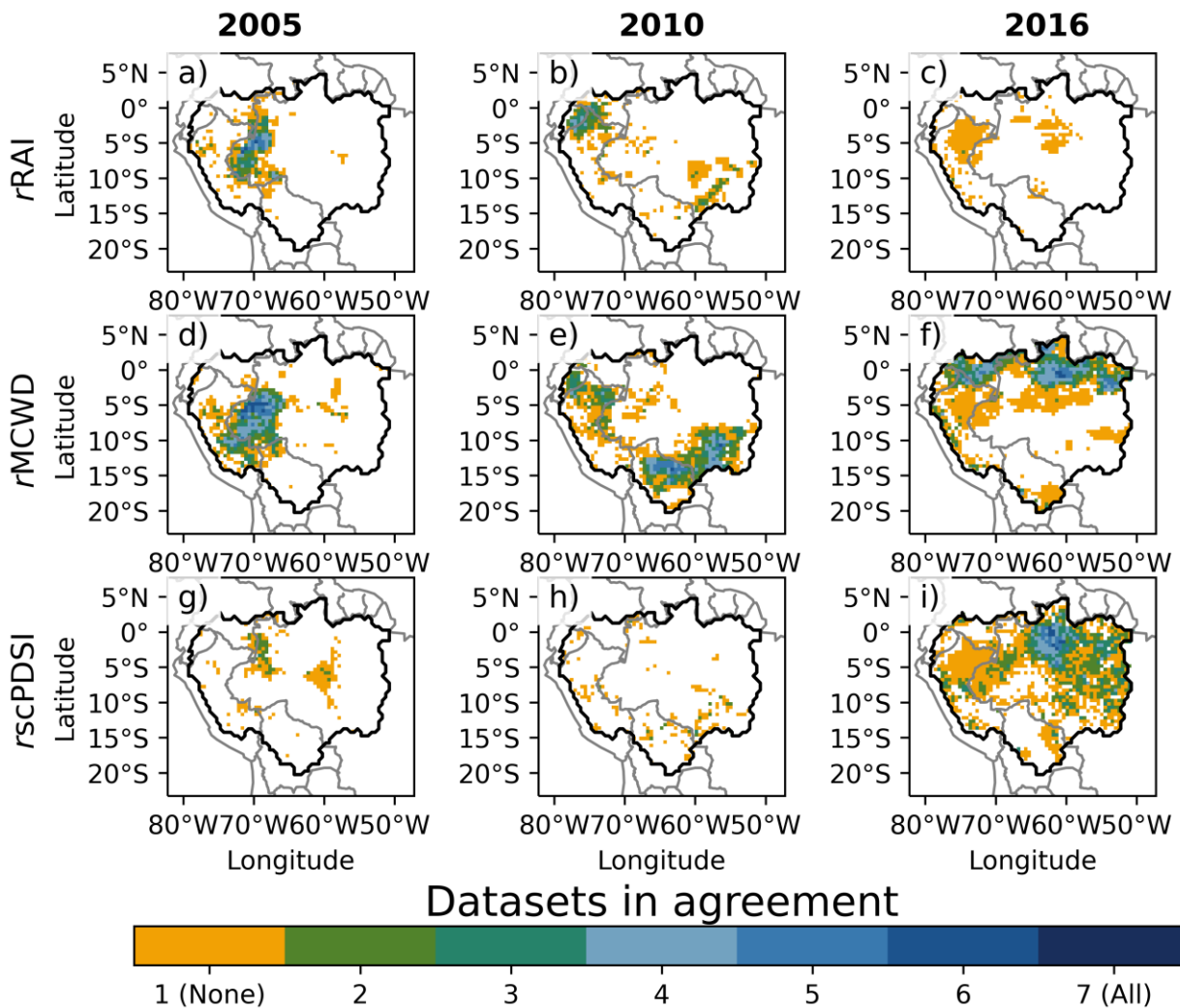
Figure 5: Agreement of precipitation datasets on drought area as identified by different drought metrics. Comparison of the Amazon drought events in 2005, 2010 and 2016 (columns) vs three different drought indexes (rows): ~~ΔMCWD~~*r*MCWD (a-c), ~~scPDSI~~*r*scPDSI (d-f) and ~~rainfall anomaly~~*r*RAI (g-i). Only the area affected by severe drought stress is displayed, ~~severe drought~~which is defined ~~differently~~equally for each of the drought indices~~: ΔMCWD less than -100mm, scPDSI less than -3 and RA less than -2~~. Orange pixels indicate areas where only one dataset shows the respective drought stress ("None"). White pixels represent areas where no dataset shows any drought signal.
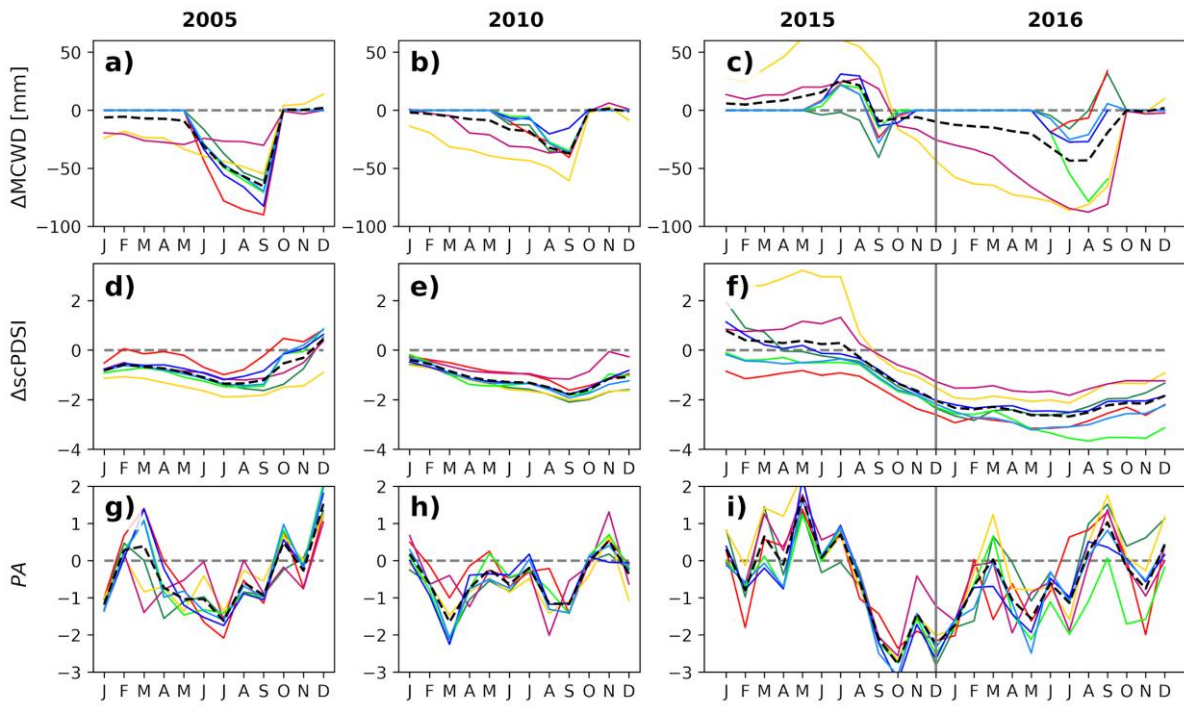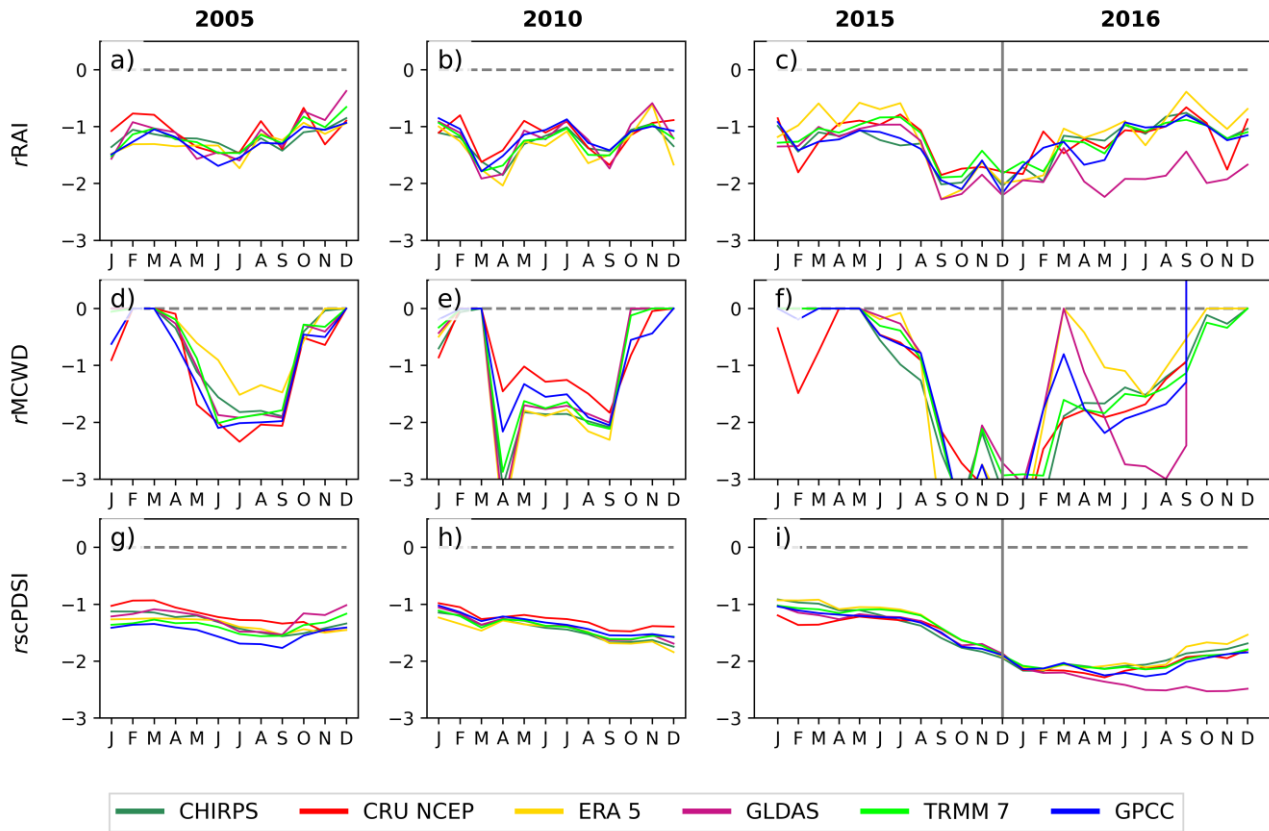
Figure 56: Monthly development of the Amazon drought events in 2005, 2010 and 2016 (columns) as described by the three different drought indices (rows): ~~ΔMCWD~~*r*MCWD (a-c), ~~scPDSI~~*r*scPDSI (d-f) and relative rainfall anomaly (~~RA~~*r*RAI, g-i). Colored lines indicate the indices of the 10% quantile of all gridcells of each of the different precipitation datasets ~~(for abbreviations see Tab. 1). RA is~~. The indices are estimated as relative deviation from a 2001 to 2016 baseline period for each month.
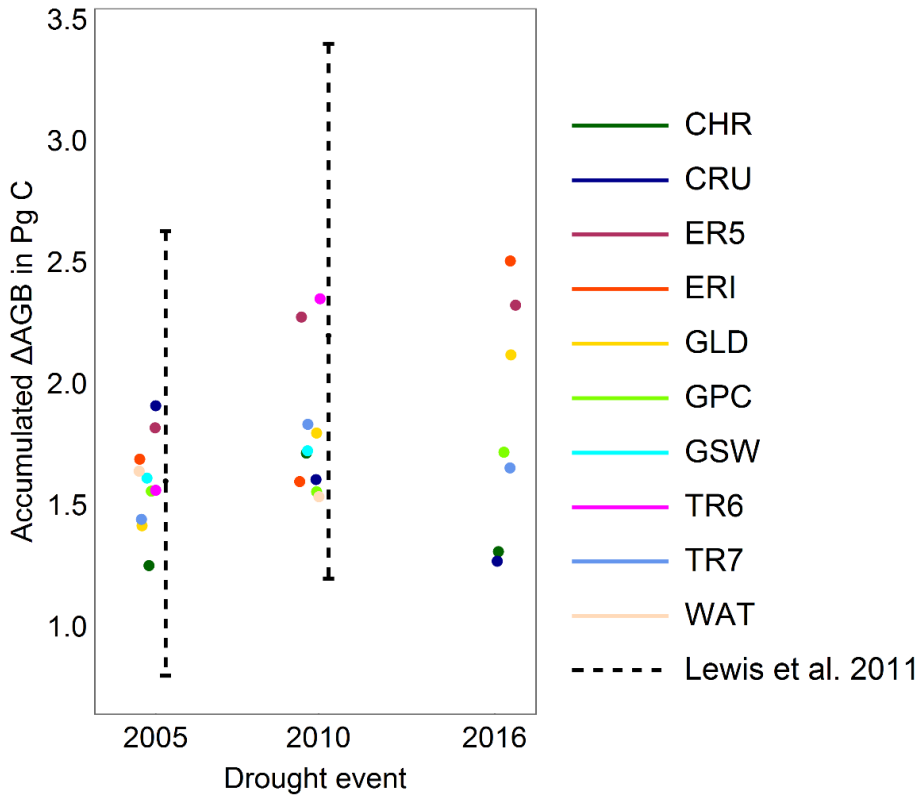
Figure 6: Impact of the 2005, 2010 and 2016 drought event on aboveground carbon biomass (AGB in Pg C). Biomass loss was calculated for each of the precipitation datasets (colored dots, for abbreviations see Tab. 1) based on a linear relation between biomass loss and ΔMCWD as proposed by Lewis

2565 **Table 1: Overview of the 10 precipitation datasets used in our study. Columns show the name of the dataset, the official abbreviation, the short abbreviation used in here, the spatial and temporal resolution and the references.**

Precipitation dataset	Abbreviation	Abbreviation (short)	Details	Resolutions	Refer
Climate Hazards group Infrared Precipitation with Stations	CHIRPS	CHR	quasi global (50°S 50°N) precipitation only merged product, based on global climatology, satellite estimates and in situ observations.	high resolution (0.05°), daily, pentadal, and monthly	Funk 2015
Tropical Rainfall Measurement Misson	TRMM v6 3b43	TR6	quasi global (50°S 50°N)	Quarter degree resolution (0.25°) daily, pentadal, and monthly	Huffm 2007
Tropical Rainfall Measurement Misson	TRMM v7 3B43	TR7	quasi global (50°S 50°N)	Quarter degree resolution (0.25°), daily, pentadal, and monthly	Huffm 2007
	CRU_NCEP V8	CNP	global	Half degree resolution (0.5°), daily, pentadal and monthly	Viovy 2017
ERA_Interim	ERA_Interim SFC12_03_T P_228	ERI	global	0.75° daily, pentadal, and monthly	Dee 20

Table 2: Total area affected by drought stress in million km² (and %) by drought index (MCWD, scPDSI and RAI) and intensity (moderate, severe and extreme) across the 10 datasets evaluated in our study (rows) for the years 2005 and 2010.

ERA5		ER5	global	Quarter degree resolution (0.25°), sub daily, daily, monthly	Alber, 2018
Global Land Data Assimilation System	GLDAS 2.1	GLD	global	Quarter degree resolution (0.25°), daily, pentadal, and monthly	Rodel, 2004
Global Precipitation Climatology Centre at Deutscher Wetterdienst	GPCC2018	GPC	global	Quarter degree resolution (0.25°), monthly	Schne... al., 20
Global Soil Wetness Project Phase 3	GSWP3	GSW	global	Half degree resolution (0.5°), daily, monthly	H. Ki... n.d.; http://...u-tokyo-WP3/...ml
WATCH Forcing Data (WFD) + WATCH Forcing Data methodology applied to ERA-Interim data (WFDEI)	WATCH_WFDEI	WAT	global	Half degree resolution (0.5°), daily, monthly	Weed... 2011,

		Year

Metric	Dataset	2005 $\Delta MCWD < -150mm$ (extreme)	2005 $\Delta MCWD < -100mm$ (severe)	2005 $\Delta MCWD < -25mm$ (moderate)	2010 $\Delta MCWD < -150mm$ (extreme)	2010 $\Delta MCWD < -100mm$ (severe)	2010 $\Delta MCWD < -25mm$ (moderate)
$\Delta MCWD$	CHR	0.0 (0%)	0.4 (6%)	3.1 (52%)	0.2 (3%)	0.9 (14%)	3.8 (63%)
$\Delta MCWD$	CRU	0.7 (12%)	1.3 (22%)	3.1 (53%)	0.2 (3%)	0.7 (12%)	3.6 (61%)
$\Delta MCWD$	ER5	0.1 (2%)	0.7 (13%)	4.2 (71%)	0.3 (5%)	1.3 (23%)	4.6 (78%)
$\Delta MCWD$	ERI	0.3 (4%)	1. (17%)	3.5 (59%)	0.3 (5%)	1. (17%)	3.2 (54%)
$\Delta MCWD$	GLD	0.3 (5%)	0.9 (14%)	2.8 (46%)	0.1 (2%)	1.1 (18%)	3.9 (65%)
$\Delta MCWD$	GPC	0.4 (7%)	1. (17%)	2.8 (47%)	0.3 (5%)	1.0 (16%)	3.1 (52%)
$\Delta MCWD$	TR6	0.2 (4%)	0.9 (15%)	3.2 (55%)	0.4 (6%)	1.7 (28%)	4.5 (76%)
$\Delta MCWD$	TR7	0.3 (4%)	0.7 (12%)	3. (51%)	0.2 (3%)	1.1 (18%)	3.9 (65%)
$\Delta MCWD$	GSW	0.5 (8%)	1.0 (17%)	2.9 (48%)	0.3 (5%)	1.1 (18%)	3.5 (58%)
$\Delta MCWD$	WAT	0.5 (8%)	1.1 (18%)	2.9 (49%)	0.2 (4%)	0.9 (15%)	3.3 (55%)
		$scPDSI < -4$ (extreme)	$scPDSI < -3$ (severe)	$scPDSI < -2$ (moderate)	$scPDSI < -4$ (extreme)	$scPDSI < -3$ (severe)	$scPDSI < -2$ (moderate)
scPDSI	CHR	0.2 (3%)	1.2 (20%)	2.5 (42%)	0.2 (3%)	2. (34%)	3.2 (55%)
scPDSI	CRU	0.3 (4%)	1.5 (26%)	2.3 (38%)	0.1 (2%)	2. (33%)	3.1 (52%)
scPDSI	ER5	0.1 (1%)	1.1 (18%)	2.8 (46%)	0.1 (1%)	1.6 (27%)	3.1 (52%)
scPDSI	ERI	0.0 (1%)	0.8 (13%)	1.7 (29%)	0. 0(1%)	1.2 (20%)	2.1 (35%)
scPDSI	GLD	0.2 (3%)	1.0 (16%)	1.9 (32%)	0.2 (3%)	2.9 (50%)	4.2 (71%)
scPDSI	GPC	0.1 (2%)	1.5 (25%)	2.6 (43%)	0.1 (3%)	1.9 (32%)	3. (51%)
scPDSI	TR6	0.3 (5%)	1.5 (25%)	2.8 (48%)	0.2 (3%)	1.9 (32%)	3.2 (54%)
scPDSI	TR7	0.3 (5%)	1.5 (25%)	2.8 (48%)	0.2 (3%)	1.9 (32%)	3.2 (54%)
scPDSI	GSW	0.2 (3%)	1.6 (26%)	2.6 (44%)	0.2 (3%)	1.8 (31%)	3.1 (52%)
scPDSI	WAT	0.2 (3%)	1.5 (26%)	2.6 (44%)	0.2 (3%)	1.8 (30%)	3. (51%)
		$RA < -3$ (extreme)	$RA < -2$ (severe)	$RA < -1$ (moderate)	$RA < -3$ (extreme)	$RA < -2$ (severe)	$RA < -1$ (moderate)
RA	CHR	0.3 (6%)	1.2 (20%)	3.1 (52%)	0.2 (3%)	1. (17%)	3.6 (60%)
RA	CRU	0.1 (2%)	0.6 (9%)	1.8 (29%)	0.1 (1%)	1. (17%)	3. (50%)

RA	ER5	0.3 (4%)	1.1 (18%)	2.9 (49%)	0.4 (6%)	1.7 (28%)	4.2 (71%)
RA	ERI	0.6 (10%)	1.1 (18%)	2.5 (42%)	0.2 (3%)	1.0 (16%)	2.7 (45%)
RA	GLD	0.2 (4%)	0.7 (12%)	1.7 (29%)	0.6 (9%)	1.2 (21%)	3.4 (57%)
RA	GPC	0.2 (4%)	0.7 (11%)	2.2 (36%)	0.1 (2%)	0.7 (12%)	2.7 (46%)
RA	TR6	0.1 (2%)	0.6 (11%)	2.4 (41%)	0.1 (2%)	1.3 (22%)	3.7 (63%)
RA	TR7	0.2 (3%)	0.9 (15%)	2.8 (47%)	0.2 (4%)	1.2 (20%)	3.3 (56%)
RA	GSW	0.2 (4%)	0.7 (11%)	2.1 (36%)	0.2 (3%)	0.9 (16%)	3.1 (52%)
RA	WAT	0.3 (4%)	0.7 (12%)	2.2 (37%)	0.1 (2%)	0.8 (13%)	2.8 (47%)

2600

Table 3: Total area affected by drought in million km² (and %) by drought index (MCWD, scPDSI and RAI) and intensity (moderate, severe and extreme) across the 10 datasets evaluated in this study (rows) for the year 2016. TR6, GSW and WAT are missing from this calculation as their timespan ends before 2016.

Metric	Dataset	2016 ΔMCWD < −150mm (extreme)	2016 ΔMCWD < −100mm (severe)	2016 ΔMCWD < −25mm (moderate)
ΔMCWD	CHR	0.4 (6%)	0.8 (13%)	2.4 (40%)
ΔMCWD	CRU	0.3 (5%)	0.7 (11%)	2.4 (41%)
ΔMCWD	ER5	0.7 (12%)	1.7 (28%)	4.1 (69%)
ΔMCWD	ERI	1.1 (18%)	1.8 (30%)	3.8 (63%)
ΔMCWD	GLD	0.5 (8%)	1.6 (27%)	3.6 (61%)
ΔMCWD	GPC	0.3 (6%)	0.9 (15%)	3.2 (54%)
ΔMCWD	TR7	0.4 (7%)	0.9 (15%)	3.2 (54%)
		scPDSI < −4 (extreme)	scPDSI < −3 (severe)	scPDSI < −2 (moderate)
scPDSI	CHR	0.3 (4%)	2.3 (38%)	3.3 (56%)
scPDSI	CRU	0.3 (5%)	2.6 (45%)	3.7 (62%)
scPDSI	ER5	0.3 (5%)	2.1 (35%)	2.9 (48%)
scPDSI	ERI	0.5 (9%)	2. (34%)	2.7 (46%)
scPDSI	GLD	0.9 (15%)	3.7 (62%)	4.2 (70%)

		$RA < -3$ (extreme)	$RA < -2$ (severe)	$RA < -1$ (moderate)
scPDSI	GPC	0.4 (7%)	2.3 (39%)	3.2 (55%)
scPDSI	TR7	0.6 (11%)	3.1 (52%)	4.2 (71%)
RA	CHR	0.0 (0%)	0.1 (2%)	0.5 (8%)
RA	CRU	0.0 (0%)	0.0 (0%)	0.3 (5%)
RA	ER5	0.0 (0%)	0.0 (0%)	0.5 (9%)
RA	ERI	0.0 (0%)	0.0 (1%)	0.9 (15%)
RA	GLD	0.6 (10%)	1.8 (30%)	3.2 (54%)
RA	GPC	0.0 (0%)	0.0 (0%)	0.7 (12%)
RA	TR7	0.0 (0%)	0.1 (1%)	0.9 (14%)